DEVELOPMENT OF SILICA FIBER REINFORCED POLYBENZOXAZINE COMPOSITES FILLED WITH ALUMINA PARTICLES AS ABLATIVE MATERIALS

A THESIS SUBMITTED TO
THE GRADUATE SCHOOL OF NATURAL AND APPLIED SCIENCES
OF
MIDDLE EAST TECHNICAL UNIVERSITY

BY

İBRAHİM EGEMEN KÜÇÜK

IN PARTIAL FULFILLMENT OF THE REQUIREMENTS
FOR
THE DEGREE OF MASTER OF SCIENCE
IN
METALLURGICAL AND MATERIALS ENGINEERING

NOVEMBER 2024

Approval of the thesis:

DEVELOPMENT OF SILICA FIBER REINFORCED POLYBENZOXAZINE COMPOSITES FILLED WITH ALUMINA PARTICLES AS ABLATIVE MATERIALS

submitted by **İBRAHİM EGEMEN KÜÇÜK** in partial fulfillment of the requirements for the degree of **Master of Science** in **Metallurgical and Materials Engineering, Middle East Technical University** by,

Prof. Dr. Naci Emre Altun
Dean, **Graduate School of Natural and Applied Sciences** _____

Prof. Dr. Ali Kalkanlı
Head of the Department, **Metallurgical and Materials Engineering** _____

Assoc. Prof. Dr. Simge Çınar Aygün
Supervisor, **Metallurgical and Materials Engineering, METU** _____

Examining Committee Members:

Prof. Dr. Cevdet Kaynak
Metallurgical and Materials Eng, METU _____

Assoc. Prof. Dr. Simge Çınar Aygün
Metallurgical and Materials Eng, METU _____

Prof. Dr. Caner Durucan
Metallurgical and Materials Eng, METU _____

Assist. Prof. Dr. Irmak Sargın
Metallurgical and Materials Eng., METU _____

Prof. Dr. Ziya Esen
Dept. of Inter-Curricular Courses, Çankaya University _____

Date: 13.11.2024

I hereby declare that all information in this document has been obtained and presented in accordance with academic rules and ethical conduct. I also declare that, as required by these rules and conduct, I have fully cited and referenced all material and results that are not original to this work.

Name Last name : İbrahim Egemen Küçük

Signature :

ABSTRACT

DEVELOPMENT OF SILICA FIBER REINFORCED POLYBENZOXAZINE COMPOSITES FILLED WITH ALUMINA PARTICLES AS ABLATIVE MATERIALS

Küçük, İbrahim Egemen
Master of Science, Metallurgical and Materials Engineering
Supervisor: Assoc. Prof. Dr. Simge Çınar Aygün

November 2024, 77 pages

The aerospace industry is seeking a replacement of phenolics to use in ablative materials because of their toxicity to human health. One of the most promising candidates is polybenzoxazine materials because of their extreme heat resistance and less toxicity. This thesis introduces thermal and mechanical properties improvement of polybenzoxazine materials by manufacturing a silica fiber-reinforced polybenzoxazine composite with the incorporation of submicron sized alumina particles. The flexural and interlaminar shear strengths of the polybenzoxazine composites were successfully risen ~11% and ~27%, respectively. One of the lowest mass ablation rates of fiber-reinforced ablative composites in the literature, 0.0284 g/s, has been achieved in the oxyacetylene test by the addition of only 3 wt% submicron alumina particles into the composite. This alumina addition reduced the

ablation rate by ~15% compared to neat polybenzoxazine composite indicating increased insulation performance for alumina added polybenzoxazine composite. This promising research points out the increased mechanical properties, improved thermal durability, and reduced ablation rate of the silica fiber-reinforced polybenzoxazine composites filled with alumina particles, and this thesis proves that polybenzoxazine materials are favorable candidates for ablation/insulation materials to be used in thermal protection systems of aerospace vehicles instead of toxic phenolic based materials.

Keywords: Polybenzoxazine Composites, Alumina, Silica Fiber, Ablative, Thermal Protection Material

ÖZ

ABLATİF MALZEME OLARAK SİLİKA FİBERLE GÜÇLENDİRİLMİŞ ALUMİNA PARÇACIK KATKILI POLİBENZOKSAZİN KOMPOZİTLERİN GELİŞTİRİLMESİ

Küçük, İbrahim Egemen
Yüksek Lisans, Metalurji ve Malzeme Mühendisliği
Tez Yöneticisi: Doç. Dr. Simge Çınar Aygün

Kasım 2024, 77 sayfa

Havacılık endüstrisi fenolik bazlı ablatif malzemelerin insan sağlığına zararlı ve toksik olması nedeniyle alternatiflerini aramaktadır. Fenoliklere en büyük alternatif adaylarından birisi yüksek ısı dayanımı ve düşük toksikliği nedeniyle polibenzoksazin malzemelerdir. Bu tez içeriğinde silika elyaf kumaş ve mikron altı boyutlarda alumina parçacık içeren polibenzoksazin kompozitlerin üretilmesi ile polibenzoksazin malzemenin termal ve mekanik özelliklerinin iyileştirilmesini içermektedir. Polibenzoksazin kompozitlerin bükülme ve tabakalar arası kesme mukavemetleri başarılı bir şekilde sırasıyla yaklaşık %11 ve %27 olarak artmıştır. Literatürde yer alan elyafla güçlendirilmiş kompozitler içinde en düşük kütle ablasyon yanma hızlarından birisi olan 0.0284 g/s'lik kütle ablasyon yanma hızı polibenzoksazin kompozite sadece kütlece %3 oranında mikron altı boyutta alumina parçacık eklenmesi ile elde edilmiştir. Bu alumina katkısının yapıldığı

polibenzoksazin kompozit içeriğinde alumina bulunmayan ablatif kompozite göre %15 daha düşük ablasyon yanma hızına sahip olmuştur ve bu durum daha iyi bir yalıtım performansı göstereceğinin ifadesidir. Bu umut vaat eden araştırma alumina katkısına sahip olan silika fiber kumaşla güçlendirilmiş polibenzoksazin kompozitlerin artan mekanik özelliklerini, iyileştirilmiş termal dayanımını ve düşmüş ablasyon yanma hızını ortaya koymaktadır. Ayrıca bu tez kapsamında yapılan çalışmalar göstermektedir ki polibenzoksazin bazlı malzemeler roketler ve füzelerin motor gövdelerinde, harp başlıklarında, nozullarda ve yanma odalarında ablasyon/yalıtım malzemesi olarak fenolik bazlı malzemeler yerine kullanılma potansiyeli taşımaktadır.

Anahtar Kelimeler: Polibenzoksazin Kompozit, Alümina, Silika Fiber, Ablatif, Termal Korumu Sistemleri

Dedicated to my mother and my girlfriend

ACKNOWLEDGEMENTS

I would like to express my gratitude to my advisor Assoc. Dr. Simge Çınar Aygün for her invaluable support and guidance throughout my studies.

I would like to thank Dr. Ayşegül Hisar Telli for her contribution to my research, synthesis, and characterization of polybenzoxazine composites with her extensive keen knowledge in benzoxazines.

I would like to thank my thesis committee: Prof. Dr. Cevdet Kaynak, Prof. Dr. Caner Durucan, Assist. Prof. Dr. Irmak Sargın, and Prof. Dr. Ziya Esen for their time and help.

I would like to thank Almatis for their kind supply of alumina particles

I would like to thank my colleague Doğu Şeyda and Duygu İnce for their help with my studies.

I am excessively thankful to Beril Balkancı for her endless love and belief.

Finally, I am extremely thankful to my beloved mother who is always the supporter of my dreams.

TABLE OF CONTENTS

ABSTRACT v

ÖZ vii

ACKNOWLEDGEMENTS x

TABLE OF CONTENTS xi

LIST OF TABLES xiii

LIST OF FIGURES xiv

LIST OF ABBREVIATIONS xvi

CHAPTERS

1 INTRODUCTION 1

2 LITERATURE REVIEW 3

2.1 Polymer Matrix Composites 3

2.2 Ablative Materials 6

2.3 Ablative Polymeric Materials and Polymer Composites 8

2.4 Benzoxazine Resin 9

2.5 Polybenzoxazine Composites 11

2.6 Flame Retardant Additives 13

2.7 Alumina Particles 15

2.8 Motivation and Scope of This Work 17

3 MATERIALS AND METHODS 19

3.1 Materials 19

3.2 Characterization of Alumina Particles 20

3.3 Composite Production 22

3.4 Characterizations 27

4 RESULTS AND DISCUSSION 31
4.1 Characterization of Benzoxazine Resin 31
4.2 Characterization of Polybenzoxazine and Polybenzoxazine Composites 33
4.2.1 Mechanical Properties of the Polybenzoxazine Composites 41
4.2.2 Thermal Properties of Polybenzoxazine Composites 43
5 CONCLUSIONS 57
REFERENCES 59
APPENDICES 71
A. Autoclave Cure Cycle 71
B. Viscosity of Uncured Polybenzoxazine Resin 72
C. Water Absorption Properties 73
D. Elemental Mapping Images 75

LIST OF TABLES

TABLES

Table 2.1 Composites of polybenzoxazine and the examples of second phase 11

Table 3.1 Composite compositions studied in this work. 26

Table 3.2 The experimental conditions of the oxyacetylene test according to GJB323A-96 standard..... 29

LIST OF FIGURES

FIGURES

Figure 2.1 Schematic that depicts the pros, cons, and applications of PMCs. Reproduced from the ref. [3] 4
Figure 2.2 Schematic of ablation process of polymeric ablatives [6] 7
Figure 2.3 Schematic listing the polymeric ablatives [13] 9
Figure 2.4 Molecular structure of different types of benzoxazine monomers namely P-a, B-a, and P-ala. Reproduced from ref. [15] 10
Figure 2.5 Glass fabric reinforced polybenzoxazine composite filled with nano SiO_2. Reproduced from the ref. [19] 12
Figure 2.6 Polybenzoxazine-carbon fiber plain woven fabric composite production. a) Impregnation of fabric b) Impregnated carbon fabric c) Uncured molded laminate d) Cured composite. Reproduced from the ref [24] 12
Figure 2.7 Polymer combustion schematic [28] 13
Figure 3.1 Digital image of silica fiber fabrics used in this study 19
Figure 3.2 SEM image of the alumina particles taken with relatively high (a) and low (b) magnification 20
Figure 3.3 Particle size analysis of alumina particles with Dynamic Light Scattering (DLS)with particle sizes ranging from 200 to 570 nm 21
Figure 3.4 XRD analysis of the alumina particles 22
Figure 3.5 Cure cycle of the polybenzoxazine composites in autoclave 23
Figure 3.6 Fabrication of polybenzoxazine composite by wet lay-up method 24
Figure 3.7 Vacuum bagging of the polybenzoxazine composite 24
Figure 3.8 Neat polybenzoxazine composite after curing in autoclave 25
Figure 3.9 Finished Polybenzoxazine composites reinforced with alumina particles 25
Figure 3.10 Interlaminar shear strength test samples 28
Figure 3.11 Thermal diffusivity test samples of polybenzoxazine composites 30
Figure 4.1 The DSC thermogram of benzoxazine resin which is heated from 50 °C to 300 °C with a heating rate of 10 °C/min 31

Figure 4.2 FT-IR spectra of benzoxazine resin and polybenzoxazine synthesized via the designed curing cycle 32
Figure 4.3 Scanning Electron Microscopy images of polybenzoxazine composites along the fiber direction a) PBZ0 b) PBZ1 c) PBZ2 d) PBZ3 34
Figure 4.4 Scanning Electron Microscopy images of polybenzoxazine composites vertical the fiber direction a) PBZ0 b) PBZ1 c) PBZ2 d) PBZ3 35
Figure 4.5 Elemental mapping images of PBZ3 (Elemental mapping images of other composites can be found in Appendix D) 36
Figure 4.6 Thermogravimetric analysis of polybenzoxazine and polybenzoxazine composites 37
Figure 4.7 DTG curve of polybenzoxazine and polybenzoxazine composites 38
Figure 4.8 FTIR spectra of polybenzoxazine, PBZ0 and PBZ3..... 39
Figure 4.9 Experimental density values of the polybenzoxazine composites 40
Figure 4.10 a) Flexural strength test samples b) Three point bending test..... 41
Figure 4.11 The influence of alumina addition into the silica fiber-reinforced polybenzoxazine composites on the mechanical properties. 43
Figure 4.12 Oxyacetylene test samples according to GJB323A-96 standard 45
Figure 4.13 Oxyacetylene test equipment during ablation testing..... 45
Figure 4.14 Mass ablation rate of polybenzoxazine composites (PBZ0, PBZ1, PBZ2, and PBZ3) 46
Figure 4.15 Comparison of mass ablation rates of polybenzoxazine composites with other studies from literature 46
Figure 4.16 X-ray diffractogram of the ablated composites (PBZ0 and PBZ3) 48
Figure 4.17 The surface morphology of the polybenzoxazine composites after oxyacetylene ablation test..... 50
Figure 4.18 Elemental mapping image of PBZ3 after oxyacetylene ablation test.. 51
Figure 4.19 Thermogravimetric and derivative thermogravimetric curves of polybenzoxazine and polybenzoxazine composites..... 53
Figure 4.20 Thermal diffusivity curve of polybenzoxazine composites 55

LIST OF ABBREVIATIONS

ABBREVIATIONS

PBZ: Polybenzoxazine

P-a: phenol-aniline

B-a: bisphenol a-aniline

P-ala: phenol-allylamine

XRD: X-Ray Diffraction

SEM: Scanning Electron Microscopy

DLS: Dynamic Light Scattering

TGA: Thermogravimetric Analysis

DTG: Differential Thermogravimetric Analysis

DSC: Differential Scanning Calorimetry

FTIR: Fourier Transform Infrared Spectroscopy

ASTM: American Society for Testing and Materials

JCPDS: Joint Committee on Powder Diffraction Standards

ILSS: Interlaminar Shear Strength

TPS: Thermal Protection System

PMC: Polymer Matrix Composite

a.u.: Arbitrary Unit

PTFE: polytetrafluoroethylene

EPDM: Ethylene Propylene Diene Monomer

CHAPTER 1

INTRODUCTION

To provide thrust in aerospace thrust motors, according to Newton's third law, the combustion gases are confined in the chamber, then they are passed through the throat and nozzle with enormous heat and pressure. To protect the aerospace thrust motors from this extremely harsh environment, ablative (a.k.a. sacrificial) materials are used in their combustion chambers, throats, and nozzles.. These ablative materials are highly endothermic, and they exhibit ablation on their outer surface degrading to form a carbonaceous layer to efficiently insulate the material under the ablated surface from the thermally harsh environment. Depending on application, fiber-reinforced polymeric composites, rigid or elastomeric heat shielding materials, and nano-structured polymeric ablatives are commonly used for ablation purposes. For the last four decades, silica fiber-reinforced phenolic composites have dominated fiber-reinforced ablative polymer composites. Phenolic resins have superior features like good thermal and chemical resistance, flame retardancy, and low water absorption, and they are inexpensive. However, traditional phenolic resins have short shelf life of their precursors and require harsh catalysts for the polymerization reaction. Moreover, phenolic resins release volatiles while curing resulting in voids in the structure making them brittle, and after curing they undergo an increased amount of volumetric shrinkage leading to dimensional instability. Most importantly, there is a health concern in the processing of phenolic resins because of the phenol and formaldehyde volatiles. Therefore, there is a growing interest in replacing phenolics from ablative composites with another polymer matrix.

The candidates to replace phenolics are thermosetting resins like bismaleimide resins, cyanate esters, and benzoxazines. Among these candidates, polybenzoxazines

have gained extreme interest in the last decade due to their unique properties, such as; infinitesimal dimensional changes upon curing, having low water absorption, being cured by just heating, extreme resistance to elevated temperatures, having a high char yield, and they do not produce toxic by-products while curing unlike phenolics. However, the polybenzoxazines and the polybenzoxazine composites are still understudied, and their full potential is not fully explored. Also, the transition from phenolics to polybenzoxazines is not yet proven worthy due to their insufficient ablative properties.

In this thesis, we studied the mechanical and thermal properties of the silica fiber-reinforced polybenzoxazine composites, focusing on their ablative properties, with the addition of sub-micron-sized alumina particles and aimed to develop ablative polybenzoxazine composites with improved thermal and mechanical properties that can replace their phenolic counterparts in thermal protection systems of high performance aerospace systems.

CHAPTER 2

LITERATURE REVIEW

2.1 Polymer Matrix Composites

Composite materials can be defined as the incorporation of two or more different materials that result in better properties than the properties of the individual materials. In general, the constituents are referred to as phases, and one phase which is continuous is called matrix phase, and the other phase which is discontinuous is the reinforcement material. Polymer matrix composites (PMCs) are the ones that the matrix is a polymer, and the reinforcement is short/long fibers, and/or particles. Polymer matrix composites possess many appealing properties like high specific strength and stiffness values due to their low densities. The advantages, disadvantages, and applications of PMCs can be examined in Figure 2.1. This special subtype of composites is employed in many different industries such as electronics, aerospace, automotive, civil applications etc. [1] [2] [3]

Figure 2.1 Schematic that depicts the pros, cons, and applications of PMCs. Reproduced from the ref. [3]

There are different sets of materials used in a polymer matrix composite. The matrix material can be thermosetting resins like epoxies, vinyl esters, polyesters, phenolics, polyimides, bismaleimide, and cyanate ester or thermoplastic materials like polyetherimide, polyetheretherketone, and poly(phynylene sulfide) depending on the application of the composite. The matrix phase of the composite serves the purpose of maintaining the reinforcing phase together, restraining mechanical and chemical failures, and providing the required geometry. The fiber reinforcement is usually chosen between glass fiber, carbon fiber and aramid fibers. The choice of fiber selection is done regarding the necessities of application and cost. For example, glass fiber is chosen when the mechanical performance necessity is not extremely high,

and the cost of glass fiber is low since it is abundant. Carbon fibers are selected when the mechanical strength is a key factor for the application due to their high specific modulus and strength. Also, carbon fibers show great performance at elevated temperatures. Aramid fibers are the answer when the impact resistance and toughness are the primary properties for the composite system. The fiber selection can be extended to ultra-high-molecular weight polyethylene, boron, and silicon carbide fibers. Moreover, there is a trend for the usage of natural fibers in composite applications like hemp and jute fibers. [1] [3]

There are some challenges for PMCs. One of the biggest challenges is the reliance on petroleum. It is known that most of the polymers that are commonly used are petroleum based, which is a limited source. Also, there is the renewability and recyclability problem of thermosetting polymers. The solution to this problem is the usage of biopolymers that have exhibited a huge number of applications. [3] [4] Another challenge is about the environmental damage polymer matrix composites cause. The hazardous air pollutants from certain volatile organic compounds and autoclave generated nitrogen oxides are released while the polymer matrix composites are manufactured or repaired. Moreover, the hazardous waste produced from disposal of expired polymer materials and contaminated scrap materials. The elimination of this problem can be achieved through the introduction of non-autoclave processing of composites and using thermoplastics instead of thermosetting polymers. [5]

2.2 Ablative Materials

Thermal Protection Systems abbreviated as TPSs are significant elements in the aerospace industry. According to the environment they work in, many different types and formulations of these materials are developed. These systems protect the structure which undergoes extremely elevated temperatures such as war heads, missiles, and nozzles etc. Depending on the working function, these TPSs can be classified into two subclasses as non-ablative and ablative materials. [6] [7]

Non ablative materials shield the elevated heat flux by re-radiation phenomenon, and the examples for this special material subclass include ceramics and metals generally. Non ablative thermal protection system materials tend to be used when the hyperthermal environment is relatively mild. [6]

Ablative materials are also known as sacrificial materials. They are highly endothermic, and they exhibit ablation on their outer surface degrading to form a carbonaceous layer to efficiently insulate the material under that ablated surface from the thermally harsh environment, and the schematic of ablation process is given in Figure 2.2. [8] Ablative material examples can be listed as the three main material classes (metals, ceramics, and polymers) and composites. For metal ablative materials, tungsten, molybdenum, and rhenium, which can perform well in aggressive thermal and chemical environments like solid rocket motor chambers and throats, can be shown as examples. [6] When the extremely high working temperatures of rocket propellants exceed the melting point of tungsten (~3422 °C) [9], ceramics and ceramic composites which can withstand the higher levels of temperatures are employed. Ceramic oxides such as hafnium oxide (HfO_2), Zirconia (ZrO_2), Yttria (Y_2O_3), Alumina (Al_2O_3), and carbides such as Boron Carbide (B_4C), Silicon Carbide (SiC), Zirconium Carbide (ZrC) were employed as ablative materials due to their high melting point. Furthermore, there is graphite which can be used as

an ablative material. Graphite has the solid-liquid-vapor triple point at 10.8±0.2 MPa pressure and ~ 4330±300 °C. Also, graphite has no melting point, and it sublimates at ~3620 °C at atmospheric pressure. These are the reasons why graphite is being used as an ablative material. [6] [10] [11] The polymeric ablative materials are discussed in the next section.

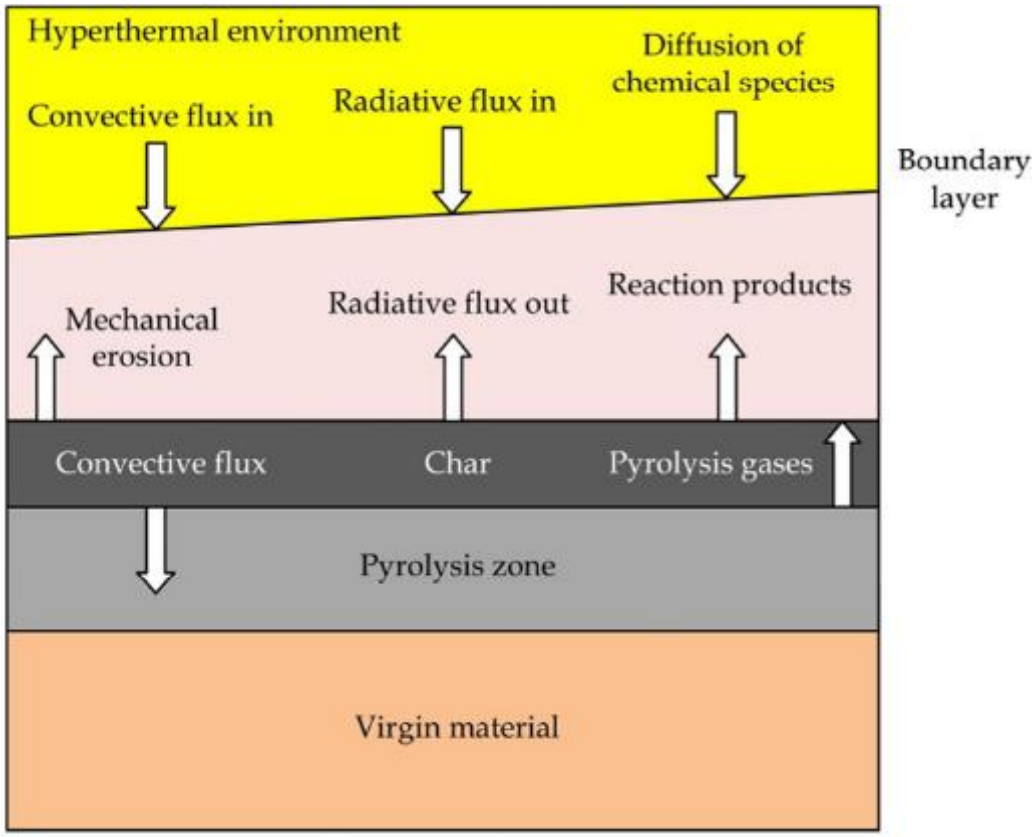

Figure 2.2 Schematic of ablation process of polymeric ablatives [6]

2.3 Ablative Polymeric Materials and Polymer Composites

Polymeric ablative materials including their composites are the most widely used subclass for ablative materials. They are mainly employed for thermal protection systems of high performance required aerospace systems. In order to provide thrust according to Newton's third law, the combustion gases are confined in the chamber, then they are passed through the throat and nozzle. There are different types of polymeric ablative materials that can be selected or developed according to the application. There can be fiber reinforced polymeric ablatives, rigid or elastomeric heat shielding materials, and nano-structured polymeric ablatives etc. For the last four decades, phenolic resins that have high char yield have been dominating the polymer ablative materials. Phenolic resins have superior features like good thermal and chemical resistance, flame retardancy, low water absorption, and being inexpensive. However, traditional phenolic resins have short shelf life of the precursors, they need harsh catalyst for the polymerization reaction, phenolic resins release volatiles while curing resulting in voids in the structure making them brittle, increased amount of volumetric shrinkage after curing leading to dimensional instability. Also, there is health concern in the processing of phenolic resins because of the phenol and formaldehyde volatiles. [12] So, there were many matrices that were tried for the purpose of developing novel ablative polymeric composites instead of phenolic resins due to their disadvantages. In addition to phenolics, thermosetting resins like polyimides, bismaleimide resins, cyanate esters, and benzoxazines can be used as a polymer matrix for ablative composites. [6] [13] [14] There are also elastomeric and thermoplastic ablative materials such as nitrile rubber, EPDM rubber, silicon rubber, polyurethane, and polytetrafluoroethylene (PTFE). [6] [14] The classification of polymeric ablative materials can be visually examined in Figure 2.3, ranging from fiber reinforced ablative materials, heat shielding materials, light weight ceramic ablators, and nano structured polymeric ablatives. [13]

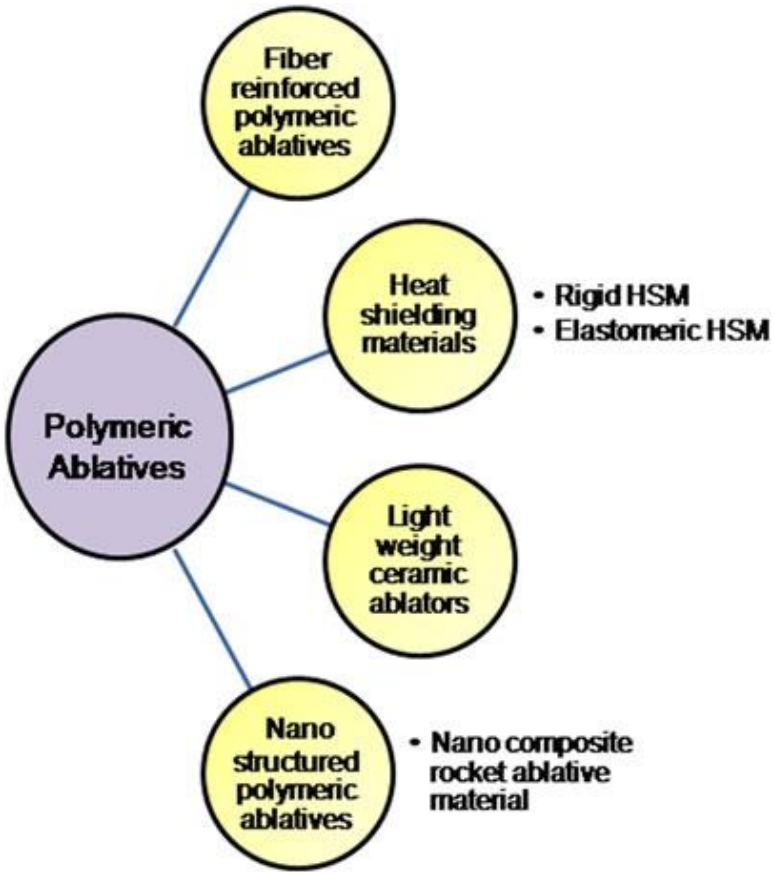

Figure 2.3 Schematic listing the polymeric ablatives [13]

2.4 Benzoxazine Resin

Benzoxazine resin is a great candidate to overcome the disadvantages of phenolic resin systems. Benzoxazine resins or addition polymerized benzoxazines, so called polybenzoxazines, possess different features that have the potential to make them superior to any other candidates to replace phenolic resins. Polybenzoxazines have only infinitesimal dimensional changes upon curing, they have low water absorption, they do not need harsh catalysts to cure, they are extremely resistant to elevated temperatures while having a high char yield, and they do not produce toxic by-products while curing. [15] [16]

The monomers of benzoxazine are synthesized with phenol, formaldehyde, and amine. Different kinds of benzoxazine monomers are possible by using different phenols and amines having various substitution groups. This allows the differentiation of polybenzoxazine properties by changing the monomers of benzoxazine at the beginning. There are many kinds of benzoxazines namely P-a (phenol-aniline) type (N-phenyl-3,4-dihydro-2H-1,3-benzoxazine), B-a (bisphenol a-aniline) type (6,6'-(propane-2,2-diyl)bis(3-phenyl-3,4-dihydro-2H-benzo[e][1,3]oxazine)), P-ala (phenol-allylamine) type (3-allyl-3,4-dihydro-2H-1,3-benzoxazine) etc., and the chemical structures of these three specific benzoxazine monomers can be found in Figure 2.4. [15]

Polybenzoxazines can be employed with different polymeric and inorganic materials that result in mixtures and blends. Rubber, polycarbonate, polyurethane, poly(ε-caprolactone), epoxy polymers, clay, silica, and alumina particles can be given as examples for polymeric and inorganic materials. [15]

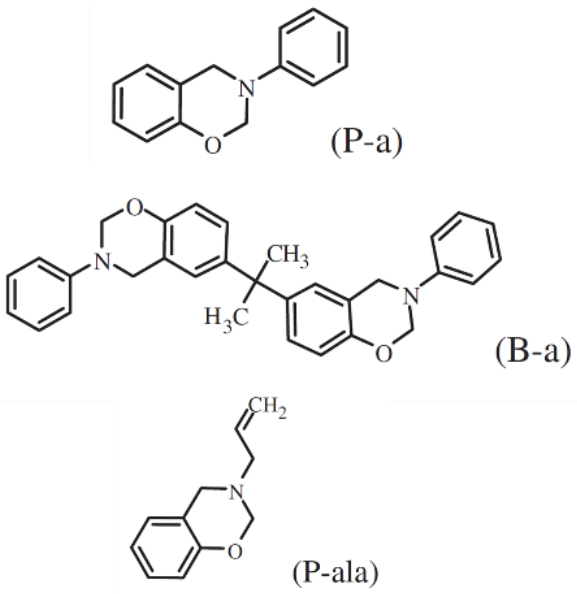

Figure 2.4 Molecular structure of different types of benzoxazine monomers namely P-a, B-a, and P-ala. Reproduced from ref. [15]

2.5 Polybenzoxazine Composites

Composites became a trend since their introduction to modern science and engineering, because of the opportunity to gain novel and improved properties from already existing materials simply by mixing. Composites are appealing because they have generally low weight, high specific strength, high specific stiffness, good fatigue resistance and good corrosion resistance. [17]

Polybenzoxazine composites attracted a lot of researchers around the globe due to the properties of the benzoxazine resin and polybenzoxazine mentioned in the previous subheading. Among the other polymer matrix composites, polybenzoxazine composites draw a lot of attention because even though the first synthesis of benzoxazine was achieved in 1940s [18], it is believed that polybenzoxazines are not deeply explored in comparison to other polymers such as epoxies, phenolics, polyesters. When compared to these polymers, polybenzoxazines have a great potential in achieving many engineering applications due to their tailorable molecular structure, and their intrinsic nature. [17] There are three main categories of polybenzoxazine composites, and Table 2.1 explains these categories. As is done in this thesis, it is possible to use a third phase in addition to polybenzoxazine matrix and the second phase. [17] [19] [20]

Table 2.1 Composites of polybenzoxazine and the examples of second phase

Composite Type	Second phase	Second phase examples
1	Other polymers	Epoxy [21], polyurethane [22] etc.
2	Inorganic particles	SiO_2 [19], TiO_2 [23], Al_2O_3 [23], CNT [24] etc.
3	Fiber reinforcements	Glass [25], carbon [1], natural fibers [1] etc.

Example composites can be investigated in Figure 2.5 and Figure 2.6 for a better understanding of the polybenzoxazine composites.

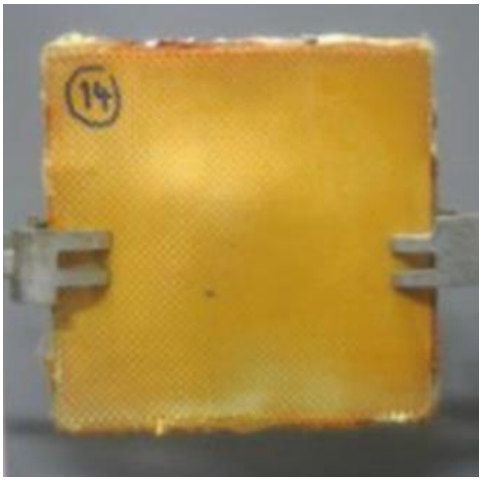

Figure 2.5 Glass fabric reinforced polybenzoxazine composite filled with nano SiO_2. Reproduced from the ref. [19]

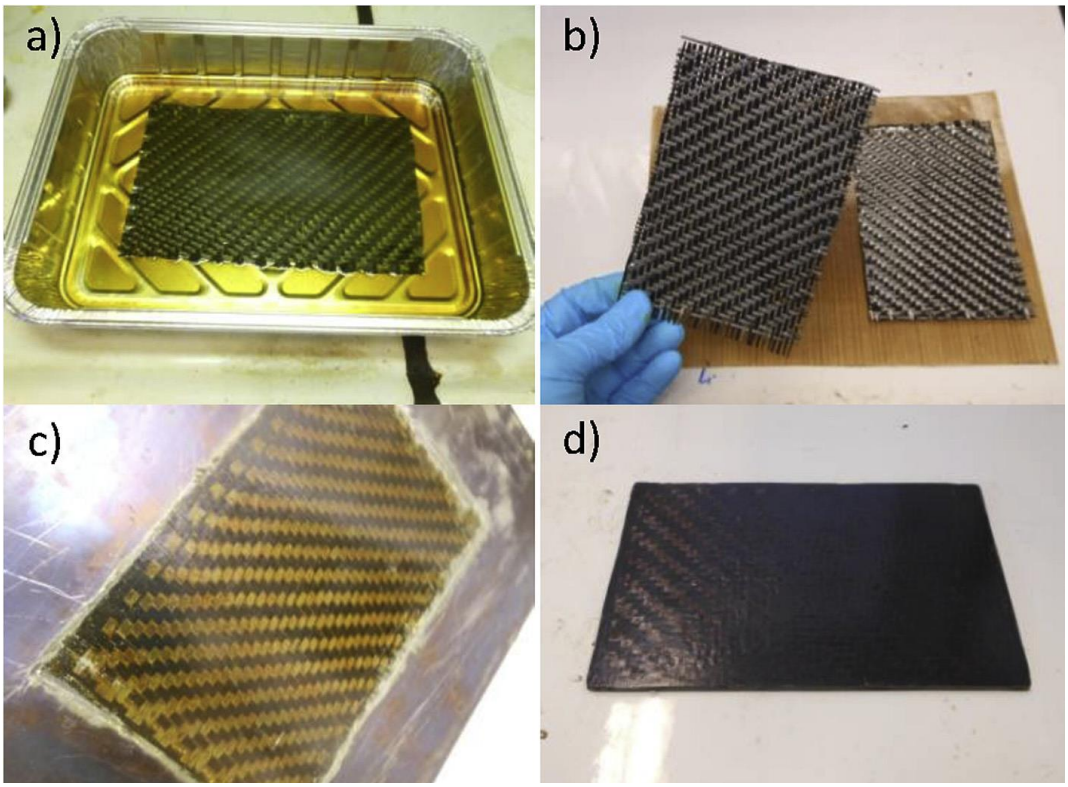

Figure 2.6 Polybenzoxazine-carbon fiber plain woven fabric composite production. a) Impregnation of fabric b) Impregnated carbon fabric c) Uncured molded laminate d) Cured composite. Reproduced from the ref [24]

2.6 Flame Retardant Additives

Because of the organic chemical structure, polymeric materials are generally extremely flammable. [26] When heated, polymers experience thermal decomposition which results in the formation of combustible gases, which burn on the surface of the polymer when exposed to heat and oxygen. The combustion of these gases creates a huge amount of heat which triggers thermal decomposition again, resulting in the continuous production of the same combustible gases. Flame retardancy can be achieved by two different approaches which are aiming gas phases and condensed phases. The gas phase approach targets capturing combustion free radicals, diluting combustible or combustion supporting gases. [27] The condensed phase approach aims at heat absorption, heat dissipation, and barrier protection effects. [28] Both phase approaches are explained in the polymer combustion schematic provided in Figure 2.7.

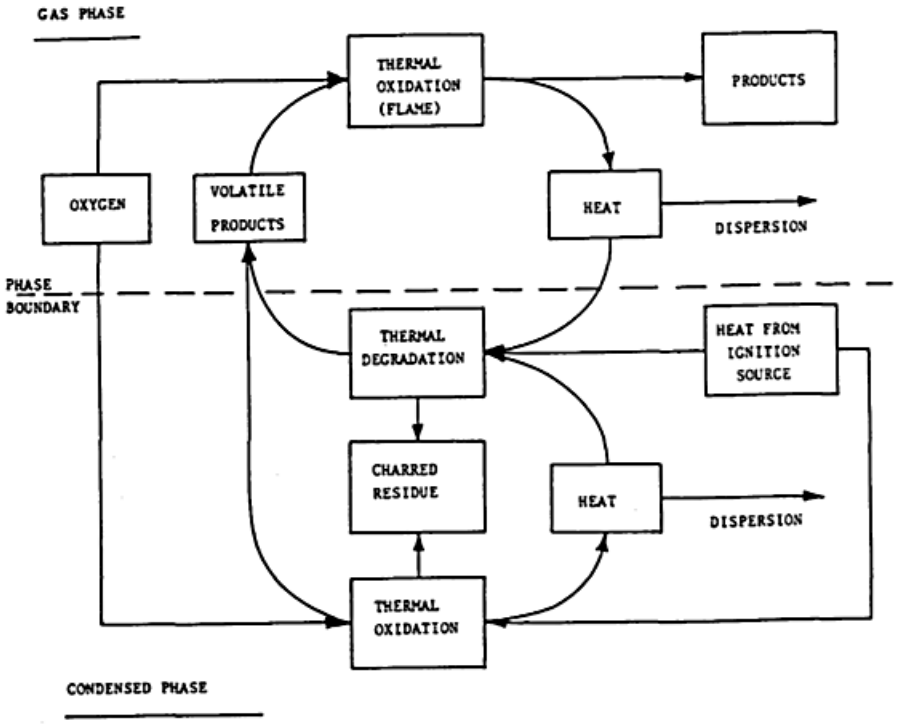

Figure 2.7 Polymer combustion schematic [28]

Flame retardant additives are the ones that are physically mixed with polymer materials. The physical mixing of flame-retardant additives does not require a complex process, and it is favorable for industrial applications. Traditional flame retardants can be classified into two categories.

The first category is inorganic flame retardants. They are employed because they are cheap, and they have low toxicity. Also, they have low smoke release which makes them 40-50 % of the mass of the flame retardants traded across the globe. [26] [29] Examples of these inorganic flame-retardants are metal hydroxides such as aluminum hydroxide, magnesium hydroxide, metal hydroxy carbonates, and metal oxides. [30] [31] When heated, these hydroxides, hydroxy carbonates, and oxides of several different metals experience endothermic decomposition resulting in the release of non-combustible gases like water vapor and/or CO_2. These non-combustible gases cause cooperated heat-sink effect, generated protective layer, and the dilution effect which produces the flame retardancy. There is also phosphorus containing inorganic flame retardants. For example, red phosphorus which has low toxicity, and high performance for flame retardancy works in both the gas and condensed phase. During the heat related thermal decomposition, gas phase flame retardancy works as produced PO· radical capturing the free radicals of combustion, and the condensed phase works as forming oxide layers of phosphoric acid which boosts the char formation which acts as a barrier for the motion of combustible gases and hindering heat transfer. [32] [33] [34]

The second category is organic flame retardants. Halogen-containing flame retardants are the generally employed organic flame retardants. Mainly they contain bromine and chlorine because other halogens possess drawbacks. They usually work in gas phase by the same phenomenon, capturing the combustion radicals. For these halogen-containing flame retardants, decabromodiphenyl oxide, dechlorane plus, and hexabromocyclododecane etc. can be given as examples. Nevertheless, due to

their toxicity, and environmental damage, halogen-containing flame retardants are prohibited globally. The research on organic flame retardants then focused on non-halogen containing flame retardants. Organophosphorus compounds including phosphines, phosphine oxides, and phosphonates etc. are used as a flame-retardant additive, and they perform both in gas and condensed phase. Moreover, nitrogen and silicon containing flame retardants are also available even though they are less efficient. [26] [35] [36]

2.7 Alumina Particles

Aluminum oxide, or alumina, is a compound of aluminum and oxygen which has the chemical formula of Al_2O_3. Alumina exists naturally in its alpha (α) crystalline phase as corundum mineral. Corundum, α-Al_2O_3, is the only form of aluminum oxide which is thermodynamically stable. Corundum can be easily found in igneous and metamorphic rocks. Corundum is one of the hardest materials in the world, its hardness is less than only diamond and a few synthetic compounds that have diamond structure. [37] Aluminum oxide can be found in its other metastable phases such as cubic γ and η phases, the hexagonal χ phase, the monoclinic θ phase, the orthorhombic κ phase and the δ phase which can be tetragonal or orthorhombic. [38] [39] Among all the other metastable phases, γ (gamma) phase alumina is the one which is the most popular in industry because of its high specific surface area, making it useful for catalytic purposes. [40] Aluminum oxide has many beneficial properties such as very high melting point, extreme hardness and strength, wear resistance, ablative properties, thermal stability, and chemical stability. [41] [42]

Alumina particles are commonly incorporated into polymeric materials to enhance thermal and mechanical properties. In the study of Paglia et al., for example, the addition of Al_2O_3 to the carbon felt-phenolic resin system resulted in a better ablation performance. This result is thought to happen because of the formation of the surface

layer of Al_2O_3 which behaved as a thermal shield. The back surface temperature of the neat and alumina containing composites are measured differently, after a certain time of exposure the temperature of the neat composite started to increase faster. Also, the back surface of that neat composite was approximately 30 °C higher than the alumina containing composite. [42] The alumina nanoparticles mixed in epoxy resin resulted in improved flexural modulus in the study of Wetzel et al., it is seen that neat resin has approximately flexural modulus value of 2.5 GPa while the 10 vol% alumina containing epoxy nanocomposite has 3.4 GPa as flexural modulus. The Charpy impact energy tests exhibited that addition of alumina particles to 1 vol% has a beneficial effect than adding no alumina. However, the addition of more than 1 vol % alumina caused a decrease in the impact energy values of the epoxy/Al_2O_3 nanocomposite system. [43] Alumina particles introduced into woven carbon fabric and phenolic resin in the study of Ali et al., in order to improve thermal and ablative properties of the composite. They have prepared composites of neat, 2%, 4%, and 6% alumina particles containing composites, and the results indicated a minor improvement in ablation resistance, whilst the thermal stability and char yield, which were determined with TGA, increased when the amount of alumina increased. [44] Polybenzoxazine containing alumina particles were studied by Kajornchaiyakul et al., and the team studied its effects on mechanical and thermal properties. They went up to 83 wt % of alumina in the polybenzoxazine, and the results are the enormous increase in the storage modulus from approximately 6 GPa to 45 GPa. Also, the glass transition temperature which was determined from the maximum of loss moduli is observed to be increased from 176 °C for neat polybenzoxazine to 188 °C for 83 wt% alumina containing polybenzoxazine. [45] As the studies given, the addition of Al_2O_3 particles to polymeric systems generally causes improvement in thermal and mechanical properties, however there are many parameters and factors one should pay attention to. For example, the concentration, the particle size, the particle morphology, and the interface between the particles and matrix system are crucial to gain such improvements.

2.8 Motivation and Scope of This Work

The literature review presented above shares the general aspects of polymeric composites and polymeric ablatives, and the urgent requirement for the replacement of the phenolics due to their toxicity both on humans and the environment. One of the candidates for the replacement of phenolic ablative materials is their polybenzoxazine-based counterparts. However, the research on polybenzoxazine materials is still in its infancy, particularly for their use as ablative materials. This thesis aims to investigate the influence of alumina particle addition into silica-fiber reinforced polybenzoxazine composites and evaluate their potential to be used as an ablative composite. To this end, first, the polybenzoxazine composites were produced from resin. Then, silica fiber-reinforced polybenzoxazine composites were prepared with additions of submicron-sized alumina particles in concentrations ranging from 0-3 wt.%. The mechanical and thermal properties of the produced composites were analyzed and compared to the ablative composites reported in the literature.

CHAPTER 3

MATERIALS AND METHODS

3.1 Materials

Phenol and aniline (P-a) based benzoxazine resin was produced by Roketsan Missiles Inc. (Turkey), and the resin was used without any further purification or any solvent addition. Silica fiber fabrics of 300 g/m^2 areal density were purchased from JSC "Polotsk-Steklovolokno" and used as received. They were woven plain type fabrics with no modification on their surfaces. Alumina particles were purchased from Almatis (CT3000 LS SG). The alumina particles were used in the polybenzoxazine composites after sieving with a 200-mesh sieve.

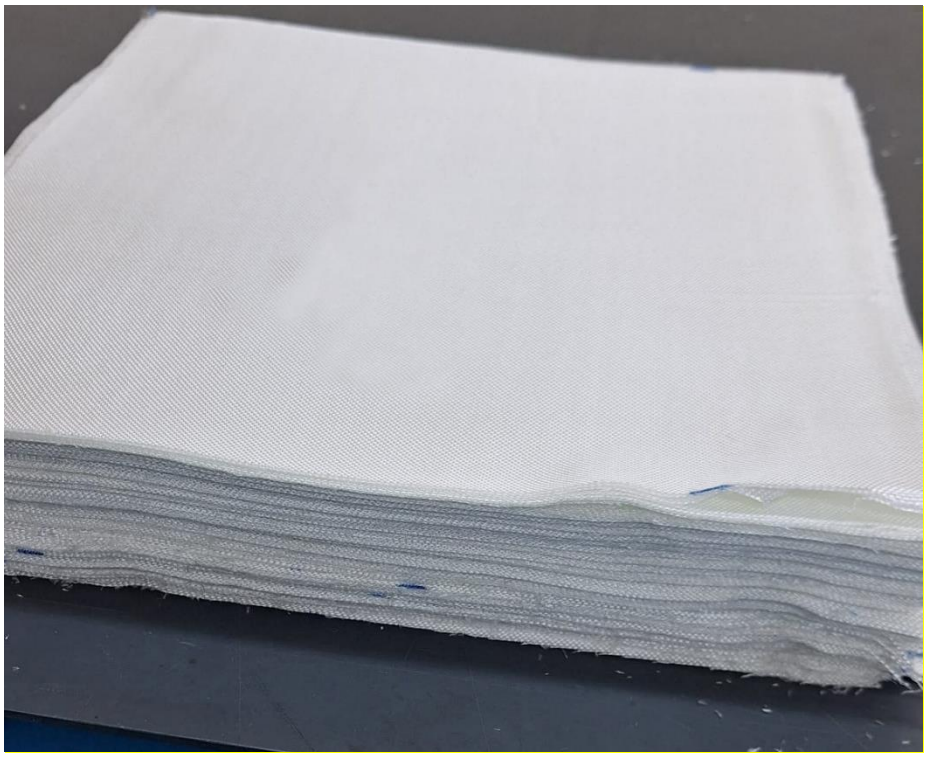

Figure 3.1 Digital image of silica fiber fabrics used in this study

3.2 Characterization of Alumina Particles

To determine the morphology of the sieved alumina particles, Scanning Electron Microscopy is used. According to the micrographs which can be seen in Figure 3.2, the alumina particles have irregular spherical morphology. The alumina particles have particle sizes around 300 nm in diameter.

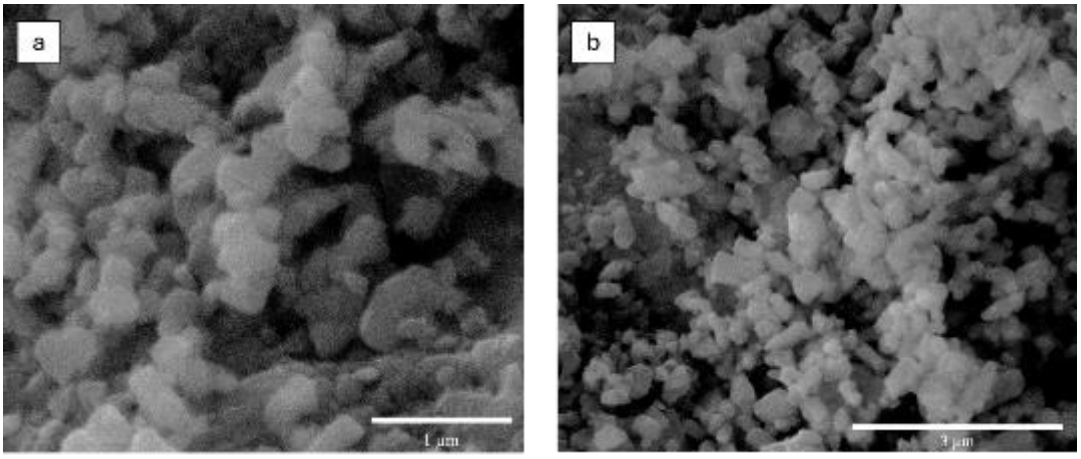

Figure 3.2 SEM image of the alumina particles taken with relatively high (a) and low (b) magnification

Then, the average particle size of alumina particles is investigated. To find the particle size of the alumina particles, Dynamic Light Scattering Analysis is conducted. The analysis is done by using the Malvern Panalytical ZetaSizer Ultra at room temperature. The alumina particles were dissolved in ethanol with a ratio of 0.03 g/ml. As it can be seen in Figure 3.3, the particle size of alumina particles resulted in a peak at 310 nm and the overall particle size of alumina particles ranges from 200 to 570 nm. The particle size results of the DLS analysis are in accordance with the SEM images. The existence of smaller and larger alumina particles was also exhibited in the SEM images.

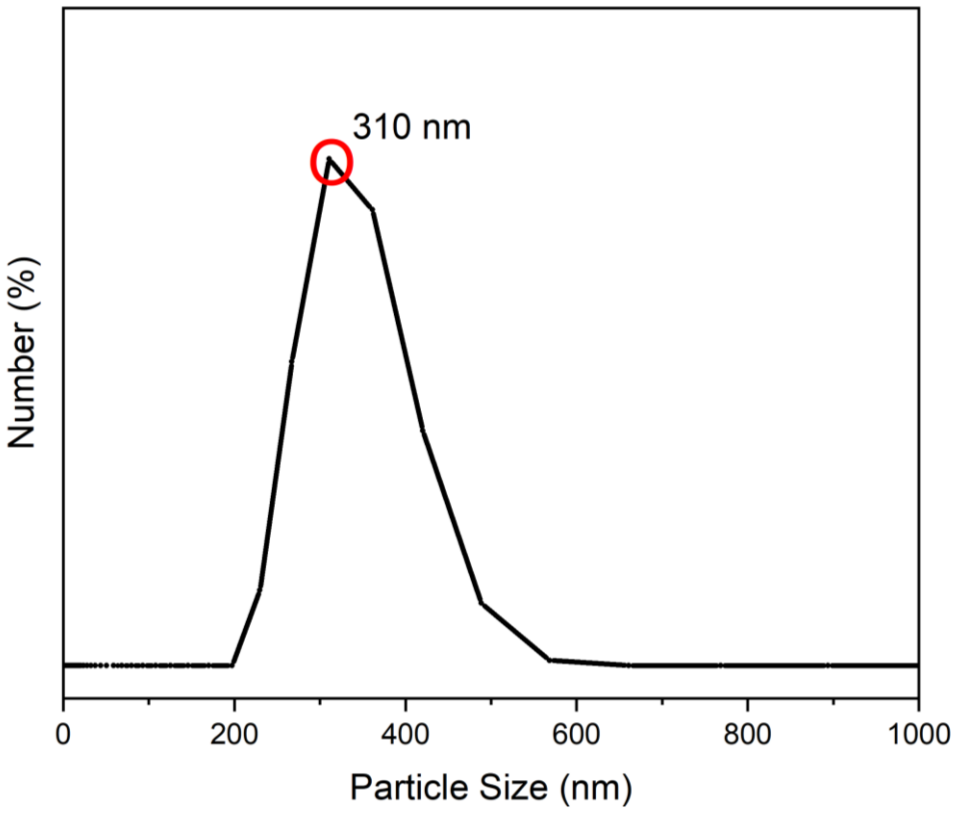

Figure 3.3 Particle size analysis of alumina particles with Dynamic Light Scattering (DLS)with particle sizes ranging from 200 to 570 nm

Then, the phase analysis of alumina particles is determined by X-Ray Diffraction analysis, and the particles are found to be α-Al2O3 according to the diffractogram provided in Figure 3.4. The Al_2O_3 particles showed peaks at 2theta angles of 25.62, 35.20, 37.82, 43.38, 46.20, 52.58, 57.52, 66.54, 68.22, and 76.90, corresponding to the (d012), (d104), (d110), (d113), (d202), (d024), (d116), (d214), (d300), and (d1010) which possess rhombohedral structure of α-alumina particles in accordance with JCPDS file no 46-1212. [46] [47] Moreover, according to the diffraction peaks, the alumina particles do not possess significant amounts of impurities.

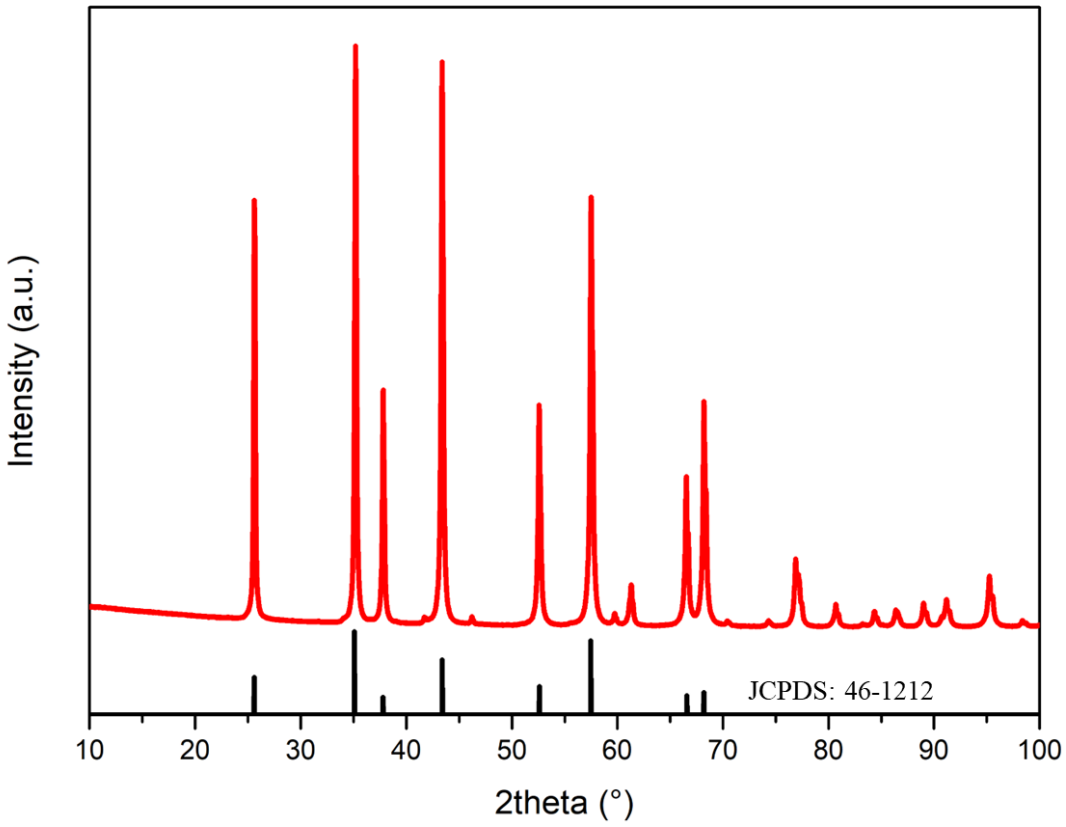

Figure 3.4 XRD analysis of the alumina particles

3.3 Composite Production

The wet lay-up method was used to produce the laminated composites. Firstly, each silica fiber fabric is cut into square pieces with edges of 250 mm. Then, one ply of silica fiber fabric was placed on top of the aluminum plate, and benzoxazine resin was poured on top of the silica fiber (Figure 3.6.a). Then, the benzoxazine resin was coated on the fabric with the help of a thin plate, and proper wetting of the fabric was ensured (Figure 3.6.b). If the composite contains alumina particles, the resin and alumina particles were stirred with a magnetic stirrer at 50 ℃ for 15 minutes at 800 rpm beforehand to enhance the homogeneity of particle dispersion in benzoxazine resin. After 100 plys were wetted with benzoxazine resin, the composites were

vacuum bagged under -0.8 bar (Figure 3.7) throughout the cure cycle and put into the autoclave to cure the benzoxazine into polybenzoxazine. A multiple-step cure cycle was employed to achieve proper curing of the composites (Figure 3.5): the system was heated to 100 ℃ in the first 50 minutes and kept at that temperature for 1 hour. Then, the temperature increased to 150 ℃ in 30 minutes and kept at that temperature for another 1 hour. After that, the temperature increased to 185 °C in 30 minutes and stayed there for 1 hour. Finally, the temperature was raised to 200 °C in 30 minutes and kept there for another 2 hours. After completion of the heating process, the system was cooled down to 50 °C in 2 hours. The pressure increased to 7 bar in the first 50 minutes of the curing process and remained constant till the last 15 minutes. The tabulated autoclave cure cycle is provided in Appendix A (Table A.1). The resulting composite is pictured in Figure 3.8 and Figure 3.9.

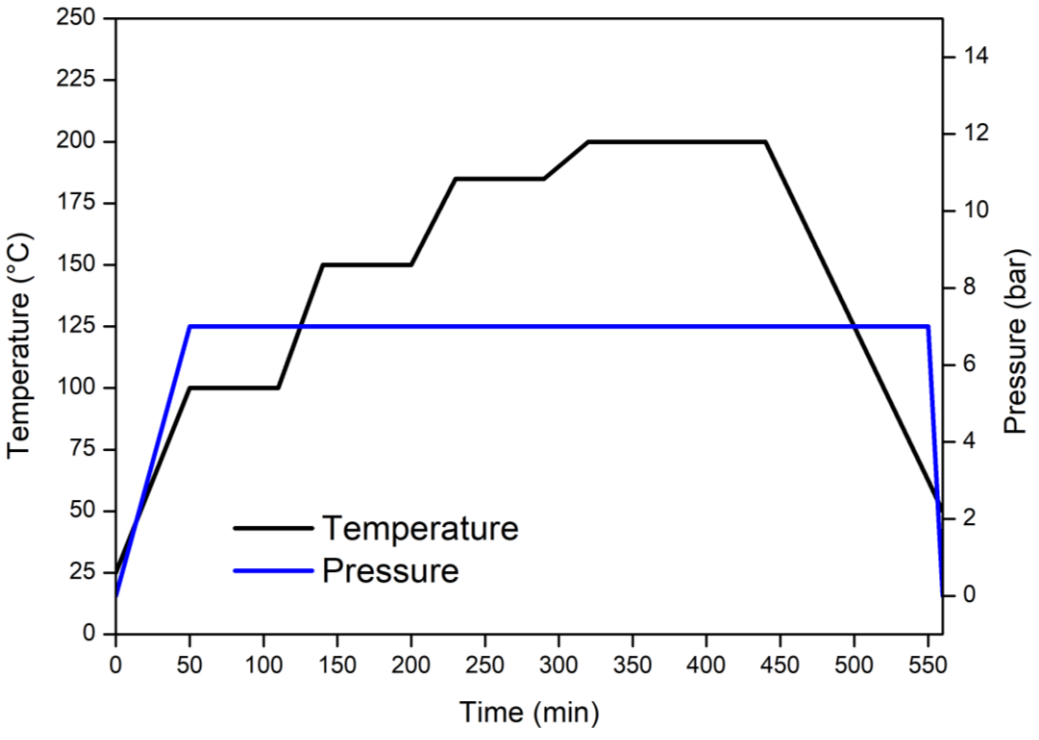

Figure 3.5 Cure cycle of the polybenzoxazine composites in autoclave

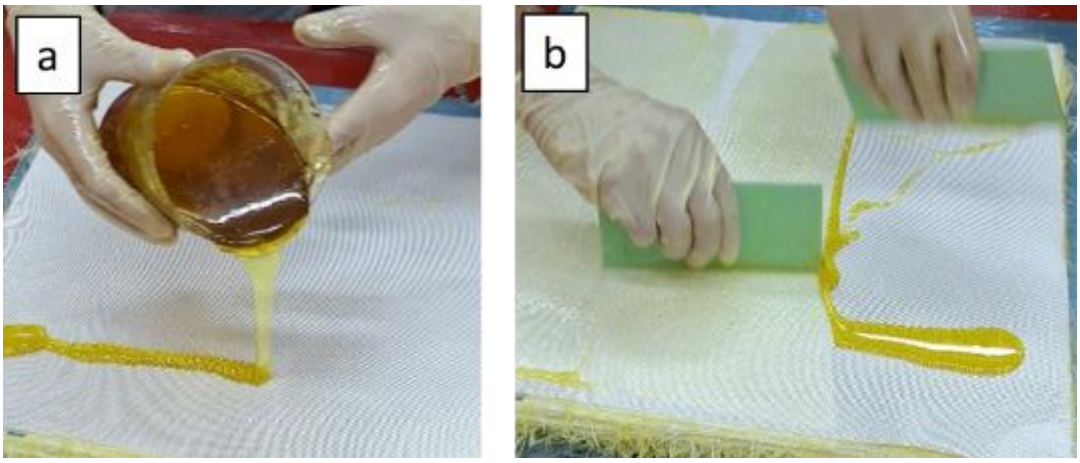

Figure 3.6 Fabrication of polybenzoxazine composite by wet lay-up method

Figure 3.7 Vacuum bagging of the polybenzoxazine composite

Figure 3.8 Neat polybenzoxazine composite after curing in autoclave

Figure 3.9 Finished Polybenzoxazine composites reinforced with alumina particles

In this study, four different laminated composites were produced to investigate the effects of the alumina particles on the thermal and mechanical properties of the composite. All composites have the same silica fiber amount, 67 wt% of the whole composite to study the influence of the alumina particles in an isolated manner. The first composite, PBZ0, was produced using 33 wt% benzoxazine resin without adding any alumina particles. The other composites were prepared using 1, 2, and 3 wt% alumina particles at benzoxazine resin's expense and labeled as PBZ1, PBZ2, and PBZ3, respectively. Further alumina addition to the benzoxazine resin increased the resin's viscosity too much to properly employ the wet lay-up method. The formulations of the composites are presented in Table 3.1. The characterizations of the composites were done on samples that are machined into required geometry and dimensions.

Table 3.1 Composite compositions studied in this work.

Composite Name	**Benzoxazine Resin (wt%)**	**Silica Fiber (wt%)**	**Alumina Particle (wt%)**
PBZ0	33	67	0
PBZ1	32	67	1
PBZ2	31	67	2
PBZ3	30	67	3

3.4 Characterizations

The morphology of the alumina particles and the distribution of components in composites was examined by scanning electron microscopy (SEM, FEINOVA NanoSEM). The elemental mappings were conducted using Tescan VEGA3 for as-prepared composites and for the composites after the ablation test. Prior to examination, both the alumina particles and polybenzoxazine composite samples were coated with gold for 3 minutes using the sputter coater Emitech SC7620.

The particle size of alumina particles are determined with Malvern Panalytical ZetaSizer Ultra using the sieved alumina particles dissolved in ethanol with the 0.03 g/mL ratio.

The phase analysis of alumina particles and the chemical composition of ablated surfaces of oxyacetylene test samples was investigated with the X-ray diffraction method using Rigaku Miniflex 600 in the scan range of 0-100° with a 0.5 °/minute scan rate.

The curing temperature of the benzoxazine resin was investigated in the temperature range of 25-300 ℃ using differential scanning calorimetry (DSC2500, TA Instruments Differential Scanning Calorimeter), and 10 ℃/min heating rate was used for the analysis.

Fourier Transform Infrared Spectrometry (FTIR) data was gathered by Bruker Tensor 27 FT-IR Spectrometer equipped with a diamond ATR accessory to examine the side groups and group changes in both benzoxazine resin and polybenzoxazine. The FTIR analysis was conducted with 32 sample scans with a resolution of 4 cm-1 between the wavelength range of 4000 to 600 cm-1.

Mechanical tests (flexural and interlaminar shear) were performed with an Instron Universal Testing Machine and repeated for five different samples for each composite type and each test. The variation was determined based on the standard deviation of the results. Flexural tests were performed on samples machined into

80×10×4 mm3 with a span length of 64 mm, and 1.7 mm/min loading speed by ASTM D790M-86. Interlaminar shear tests were conducted on samples with a T-shaped geometry with a 5 mm/min loading speed according to the GBT1450.1 standard.

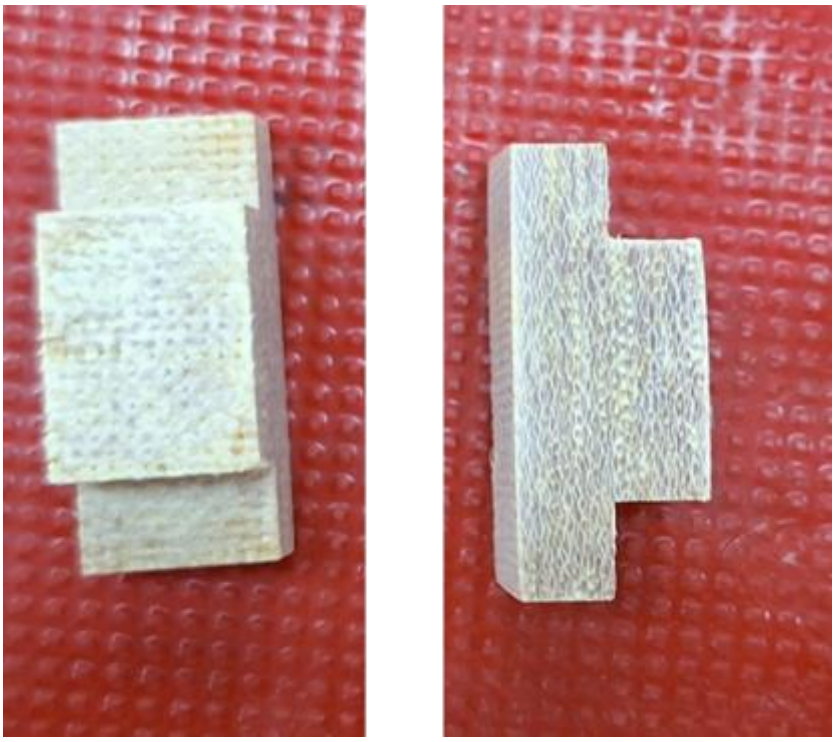

Figure 3.10 Interlaminar shear strength test samples

Oxyacetylene tests were done using specially made equipment designed for this test by GJB323A-96. The detailed test parameters are given in Table 2. The oxyacetylene test was conducted on the disk-shaped specimens, having dimensions of 30 mm diameter and 10 mm thickness. In this test, the samples were exposed to a strong oxyacetylene flame, and the mass difference of the samples before (mi) and after (mf) occurred during the test duration (Δt, 20 seconds for all the composites) were used to determine the ablation rate (Equation 1). The test was conducted on five samples for each, and the variations were calculated according to the standard deviation of the results.

$$Mass\ Ablation\ Rate\ (g/s) = \frac{m_i - m_f}{\Delta t} \quad [1]$$

Table 3.2 The experimental conditions of the oxyacetylene test according to GJB323A-96 standard

Parameters	**Value**
Oxygen gas flow rate	1512 l/h
Acetylene gas flow rate	1116 l/h
Oxygen pressure	0.4 MPa
Acetylene pressure	0.095 MPa
Distance between nozzle tip and sample	10 mm
The angle between flame and sample	90 °
The heat flux of the flame	4200 kW/m^2
Flame temperature	3000 °C

Thermal durability of polybenzoxazine and its composites were investigated using thermogravimetric analysis (TGA, TA Instruments Thermogravimetric Analyzer TGAQ500) in the temperature range of 25 – 900 °C with 10°C/min heating rate under N2 environment.

For thermal diffusivity measurements, the composite samples were machined into tiny disks of 12.7 mm in diameter with a thickness of 2 mm. These samples were placed into the instrument (TA Instruments DLF 1600) and tested under a N2 atmosphere with a 10 °C/min heating rate in the temperature range of 25 – 175 °C.

The thermal diffusivity of the samples was measured at every 25 ℃ increment according to ASTM E1461-01. The tests were repeated for three different samples for each composition.

Figure 3.11 Thermal diffusivity test samples of polybenzoxazine composites

The viscosity of the benzoxazine resin at different temperatures and with different solvents were measured with a tabletop Brookfield Rotational Viscometer, and the results are given in Appendix B.

The water absorption properties of polybenzoxazine composites were calculated. To achieve this, three cubic polybenzoxazine composites samples of 10 mm in edges are machined for each composite type, and they were weighed. Then, each cubic sample was placed inside different bottles that are filled with the same amount of pure water. After 1, 7, and 28 days, each cubic sample's mass was weighed again to realize how much water is absorbed by the composite. Then, the percentage difference between masses before and after is recorded. These results can be found in Appendix C.

CHAPTER 4

RESULTS AND DISCUSSION

4.1 Characterization of Benzoxazine Resin

In order to determine the processability and process parameters of the composite system, benzoxazine resin is characterized. The curing parameters of the polymerization reaction of benzoxazine to polybenzoxazine were determined based on the thermal and spectral analysis of benzoxazine resin. The Differential Scanning Calorimetry (DSC) analysis in Figure 4.1 showed that the exothermic curing reaction starts at 190 °C and results in a peak around 210 °C. Hence, a stepwise curing cycle with a maximum temperature of 200 °C (Figure 3.5) was designed to ensure homogeneous polymerization that takes place slowly in order not to shock the polymer.

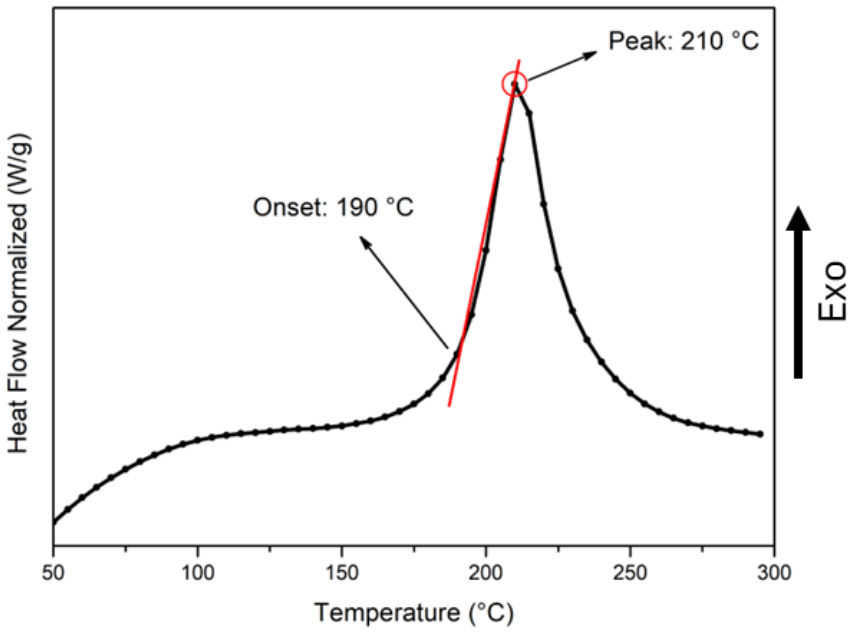

Figure 4.1 The DSC thermogram of benzoxazine resin which is heated from 50 °C to 300 °C with a heating rate of 10 °C/min

The benzoxazine is then polymerized by the cure cycle decided according to the DSC analysis. To examine the success of the polymerization, Fourier Transform Infrared Spectroscopy is conducted on benzoxazine and polybenzoxazine separately. It is known that benzoxazine is polymerized into polybenzoxazine by a ring-opening reaction of the oxazine groups of benzoxazine.[48] As observed in the FTIR analysis results in Figure 4.2, the peak around 940 cm^{-1} in benzoxazine resin's spectra, representing the benzene with attached oxazine ring, disappeared after the curing process, confirming the completion of the polymerization reaction. In addition, the absorption peaks around 1225 and 1031 cm^{-1} are due to the asymmetric and symmetric stretching peaks of C-O-C of the oxazine ring, and the absorption peaks around 1155 and 1365 cm^{-1} are attributed to symmetric and asymmetric stretching vibrations of C-N-C bonds on the oxazine ring.[14] [49] The decrease in the intensity of these peaks after the curing process supports the successful polymerization of benzoxazine into polybenzoxazine with the selected cure cycle.

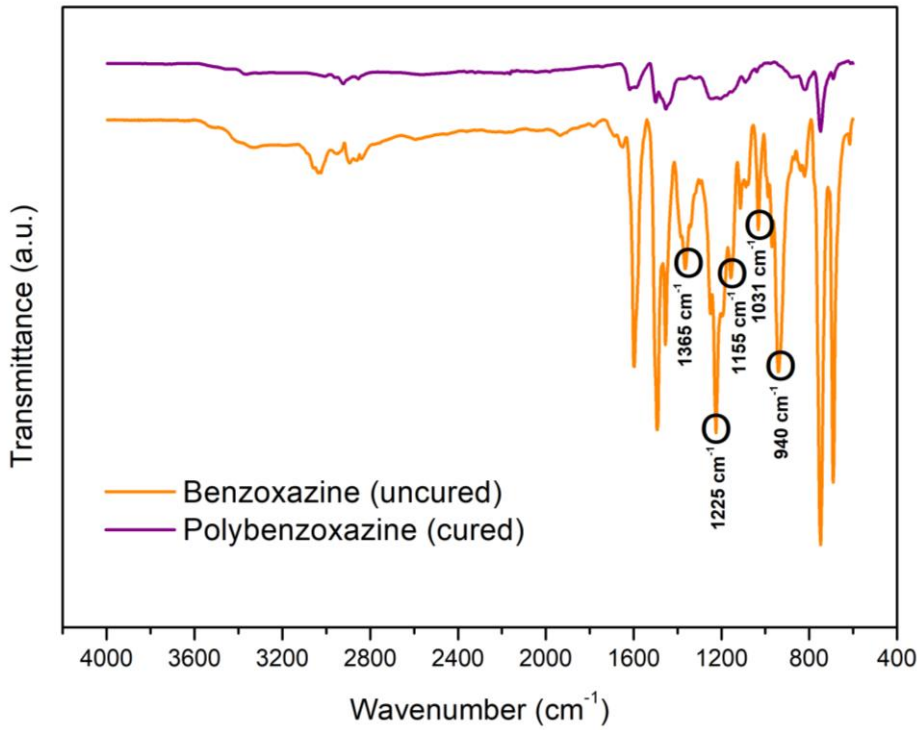

Figure 4.2 FT-IR spectra of benzoxazine resin and polybenzoxazine synthesized via the designed curing cycle

4.2 Characterization of Polybenzoxazine and Polybenzoxazine Composites

After designing the polymerization procedure and confirming that it is a suitable cure cycle, the silica fiber-reinforced polybenzoxazine composites with alumina addition were prepared using the wet lay-up method and cured following the procedures provided in Section 3.3. After the production of composites, cubic samples with edges of 10 mm were machined. Then, the distributions of fibers and alumina particles in the polybenzoxazine matrix were analyzed via SEM. As presented in Figure 4.3 and Figure 4.4, the benzoxazine resin is distributed among the silica fibers without a significant failure. Also, for the composites PBZ1, PBZ2, and PBZ3, Figures 4.3.b-d and Figures 4.4.b-d demonstrates, in addition to the fibers and the polymer matrix, the alumina particles which are dispersed in the composite can be seen. In order to evaluate the dispersion of alumina particles better, elemental mapping was conducted on these composite samples. The elemental maps of PBZ3 given in Figure 4.5 confirm that alumina particles homogeneously dispersed in the resin and show only a slight agglomeration. Addition of alumina content to polybenzoxazine composites with increasing trend from PBZ0 to PBZ3 can be demonstrated by the elemental mapping images of other composites provided in Appendix D. It is observed that benzoxazine resin is dispersed among the silica fibers in all SEM images indicating it filled most of the gaps leading to a composite that doesn't have a significant amount of porosity. The absence of significant amount of porosity is also demonstrated with density calculations which are mentioned in the next sections. It is seen that alumina particles tend to both adhere to silica fibers and blend into the benzoxazine resin well, and this situation explains the increase, which will be mentioned in the next sections, in the performance of polybenzoxazine composites which can be related to strong chemical affinity in between the matrix, fiber, and particles.

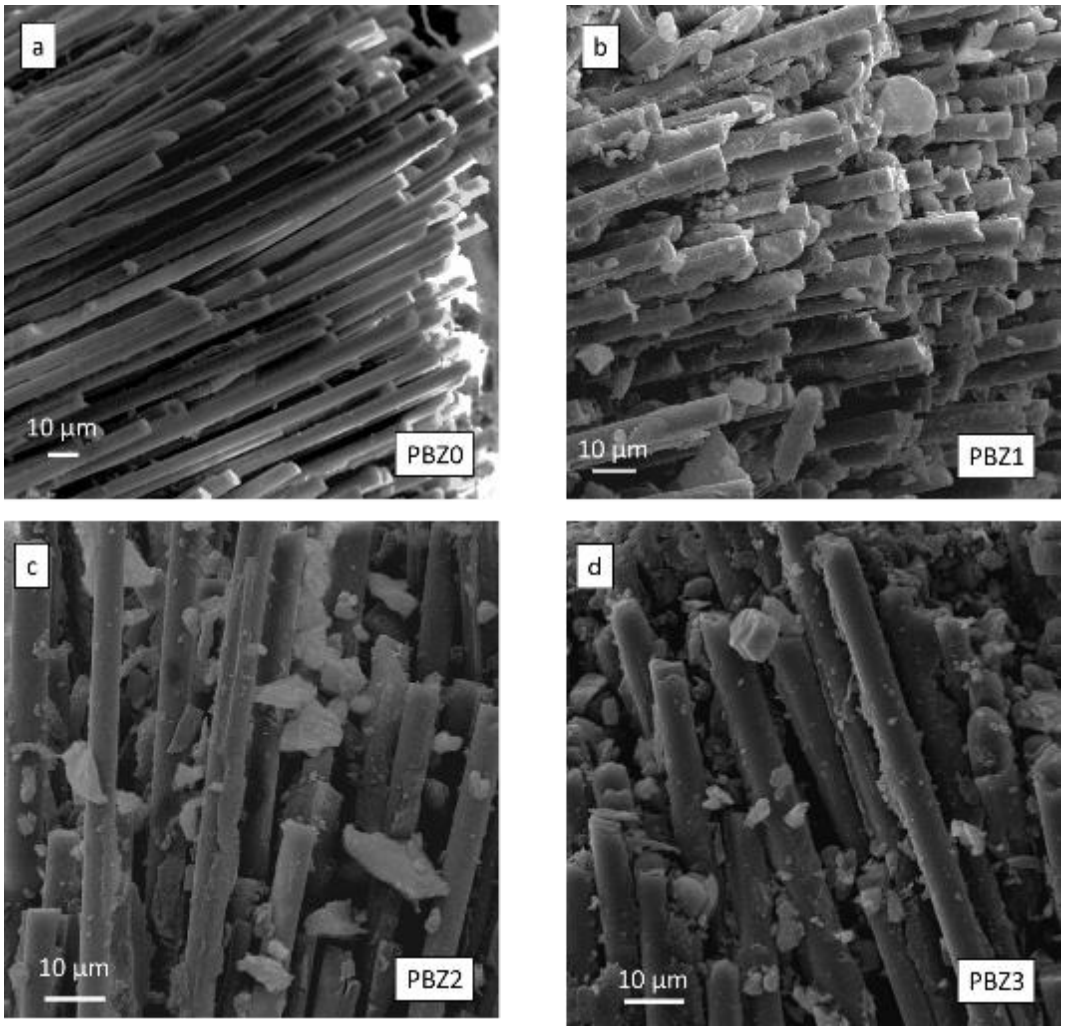

Figure 4.3 Scanning Electron Microscopy images of polybenzoxazine composites along the fiber direction a) PBZ0 b) PBZ1 c) PBZ2 d) PBZ3

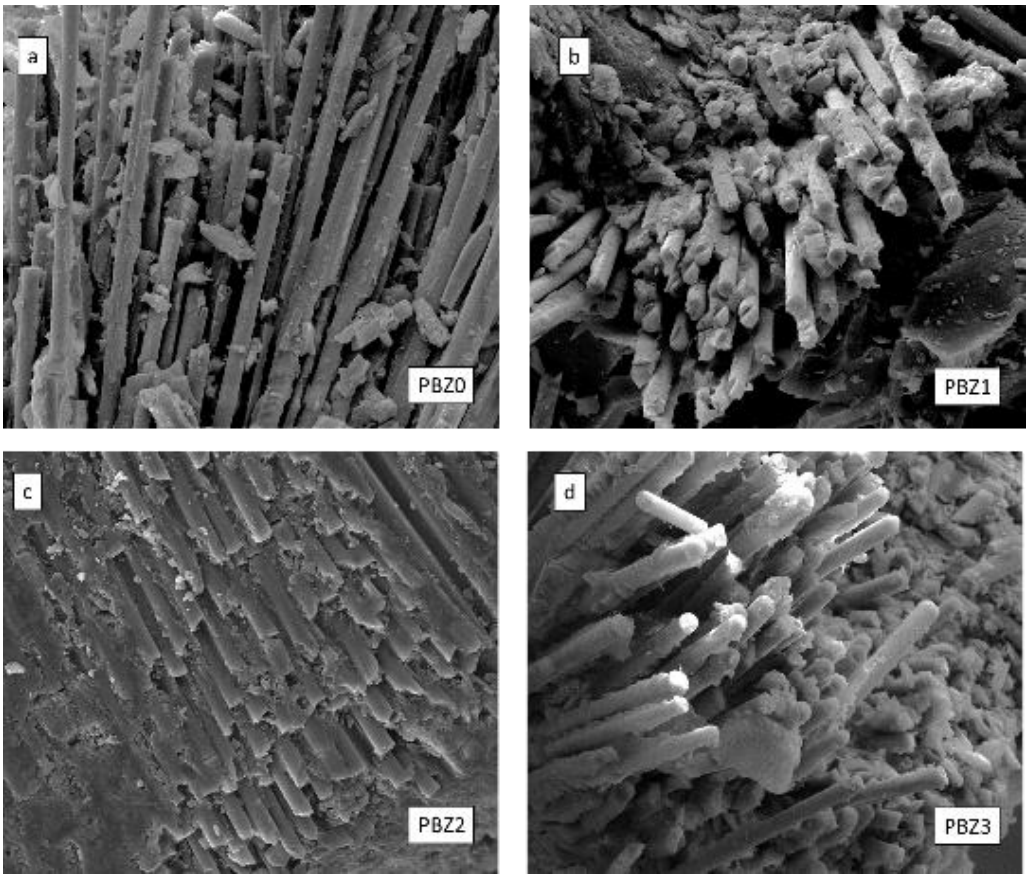

Figure 4.4 Scanning Electron Microscopy images of polybenzoxazine composites vertical the fiber direction a) PBZ0 b) PBZ1 c) PBZ2 d) PBZ3

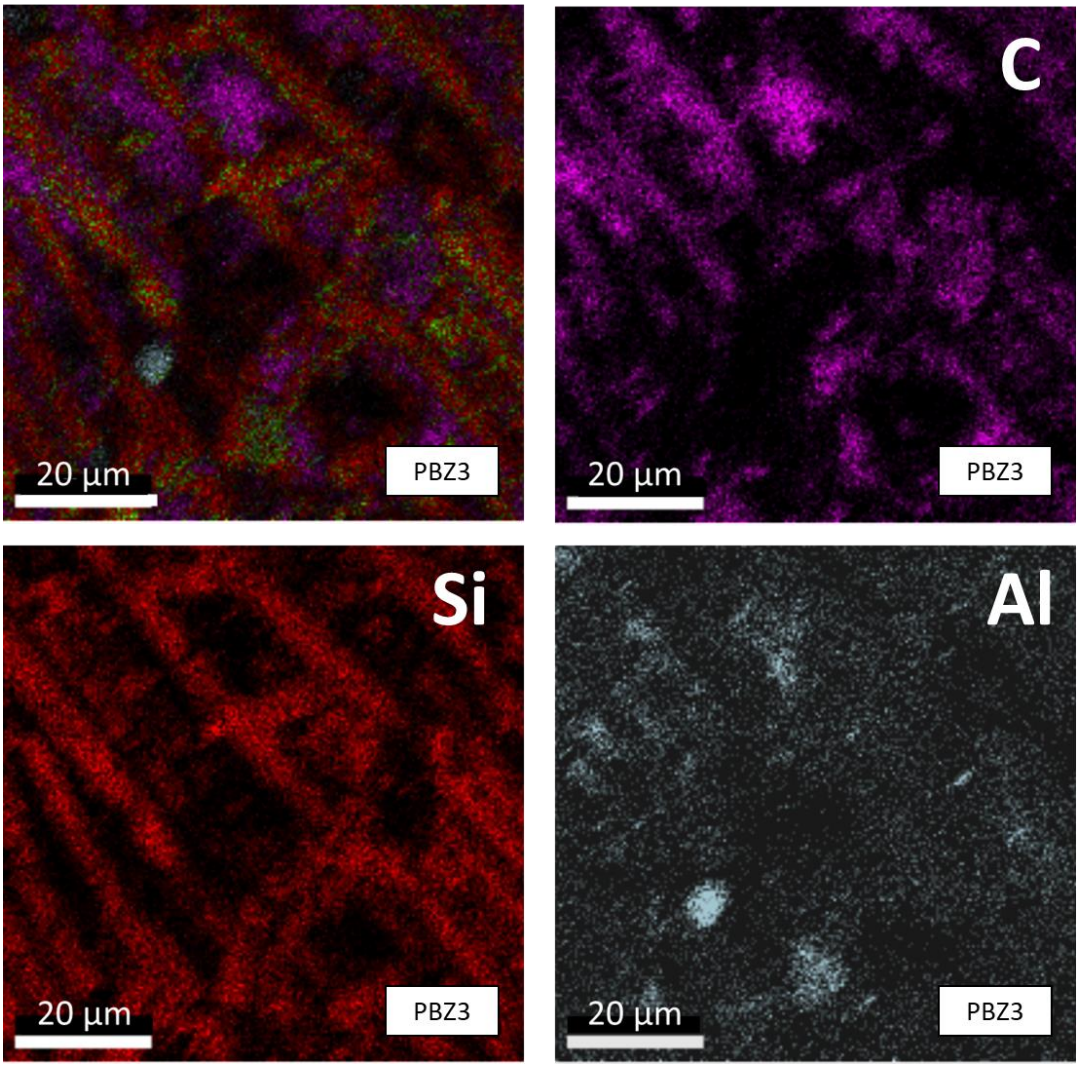

Figure 4.5 Elemental mapping images of PBZ3 (Elemental mapping images of other composites can be found in Appendix D)

In Figure 4.6 and Figure 4.7, the TGA and DTG curves of polybenzoxazine and polybenzoxazine composites can be seen respectively. When pristine polybenzoxazine polymer was exposed to this test, it is seen the degradation of the polymer begins around 200 °C and finishes approximately at 550 °C, and the thermal degradation of the polybenzoxazine takes place in two steps. The former step represents the weight loss due to the evaporation of amine groups, and the latter step represents the weight loss due to the degradation of phenolic compounds. [50] [51]

It is observed in the DTG curve that the first weight loss of polybenzoxazine, due to the evaporation of amines, around 200-300 °C is nearly concentrated around 200 °C for the polybenzoxazine composites, and finished before 220 °C. Then, the first peak of the degradation of phenolic moieties reached its fastest point around 410 °C, while for PBZ0 this reaction shifted to lower temperatures around 380 °C. Moreover, when the alumina particles are introduced to the composite, another shift to higher temperatures compared to PBZ0's, around 390 °C, is observed for the same reaction. Also, the second peak temperature of this degradation step takes place around 480 °C for polybenzoxazine polymer, however the peak temperature shifts to lower temperatures again for the polybenzoxazine composites following the same trend of the prior reaction. Both shifts of the two reactions indicate strong interfacial bonding and molecular interaction between alumina particles, silica fibers and polybenzoxazine implying the successful chemical fabrication of the composites. The effect of the amount of alumina particle in the structure to the reaction shifts could not be determined pointedly.

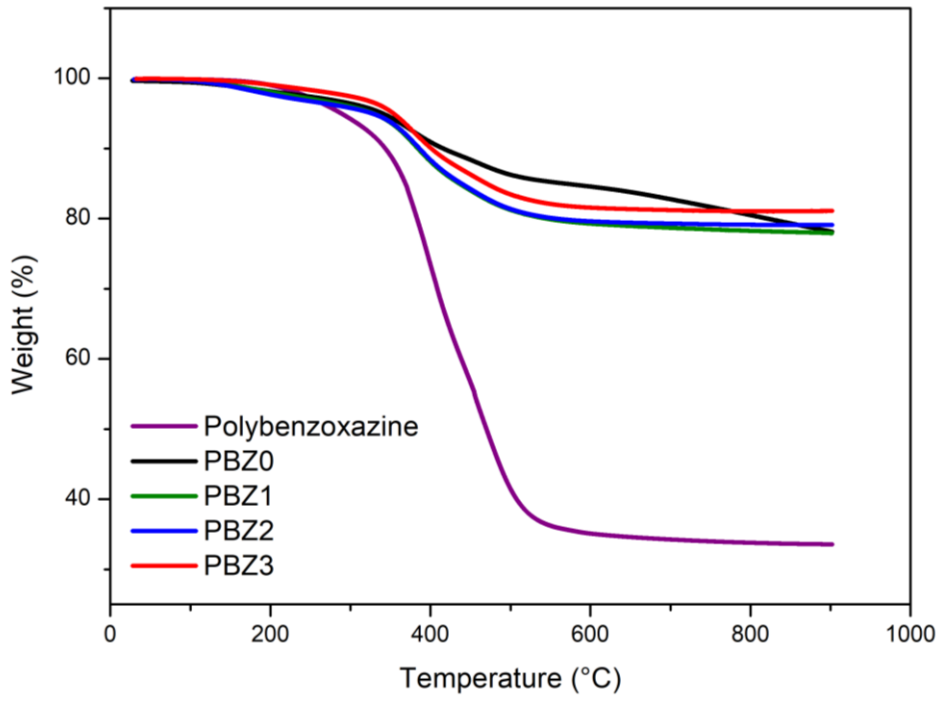

Figure 4.6 Thermogravimetric analysis of polybenzoxazine and polybenzoxazine composites

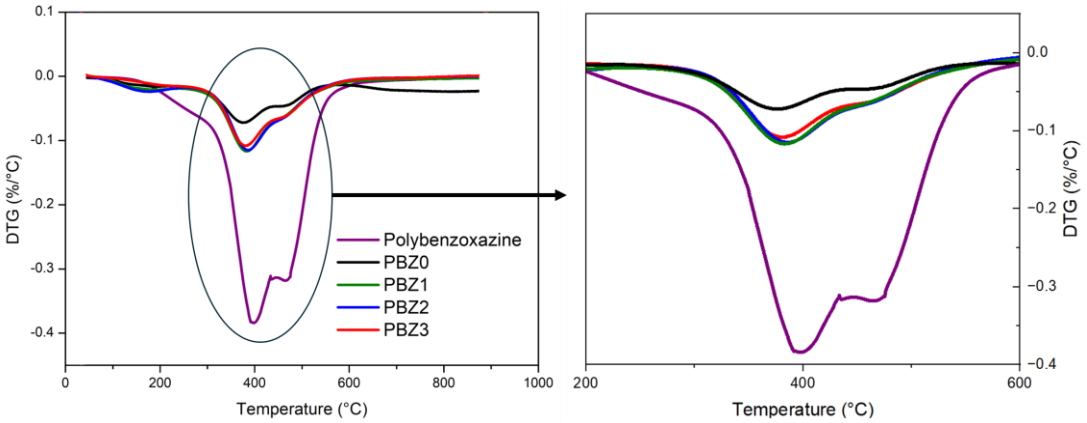

Figure 4.7 DTG curve of polybenzoxazine and polybenzoxazine composites

To further investigate the manufacturing of the composites, FTIR analysis is conducted to observe the changes that occurred to the chemical structure of polybenzoxazine when it is mixed with silica fiber and alumina particles, and it can be seen in Figure 4.8. The broad band seen for the polybenzoxazine and both composites at 3400 cm^{-1} can be assigned to symmetric stretching of hydroxyl groups. The sharp peak around 795 cm^{-1} can be related with symmetric stretching vibration of Si-O-Si which is present due to the silica fiber in PBZ0 and PBZ3. There is a strong and sharp peak around 1040 cm^{-1} for PBZ0 and PBZ3 which indicates the asymmetric stretching of the Si-O-C groups formed between the silica fiber and the polybenzoxazine in the composite which can suggest the chemical interaction between the polybenzoxazine and the silica fiber. Mora et al. [19] and Dueramae et al. [52] also stated the siloxane group (Si-O-C) is observed when they fabricated polybenzoxazine and silica containing composites. For PBZ3, there are also transmittance peaks around 640 cm^{-1} attributed to Al-O stretching, and 760 cm^{-1} attributed to Al-O torsional frequencies. [53] [54] These findings are in accordance with the 3 wt% alumina content in PBZ3. Moreover, when the sharp asymmetric peak around 1040 cm^{-1} for PBZ0 and PBZ3 is examined, it is seen that the ratio of these asymmetric is altered when alumina particles are introduced to the composite in PBZ3. It is thought that the existence of alumina particles either restrict or allow

the vibration of one of the peaks at 1040 cm^{-1}, making the overall peak to be more asymmetric. This difference between the ratios of these peaks implies a chemical interaction between the alumina particles and the Si-O-C groups has occurred, and this molecular interaction is another indication of the successful chemical composite production, instead of a simple physical blending.

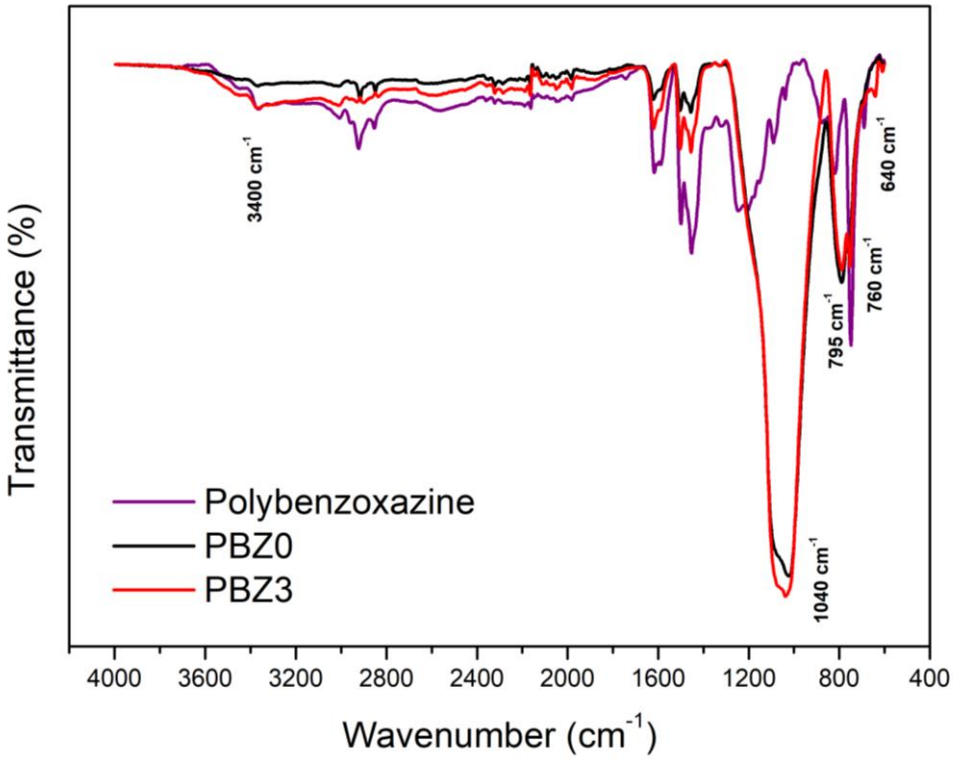

Figure 4.8 FTIR spectra of polybenzoxazine, PBZ0 and PBZ3

For an ablative composite to be preferrable, one of the significant features is its density. For thermal protection systems, the total mass of the system is a crucial parameter, and for that reason any part of the system should be lightweight. Polymer matrix composites are generally known for their lightweight nature, and polybenzoxazine composites also possess this feature. The densities of all composites, from PBZ0 to PBZ3, are measured by Archimedes method. As is depicted in Figure 4.9, the densities of the composites tend to increase with increased

alumina particles content as expected. According to the measurements, PBZ0 has 1.714 g/cm^3 density, PBZ1 has 1.752 g/cm^3 density, PBZ2 has 1.771 g/cm^3 density, and PBZ3 has 1.782 g/cm^3 density. These density values are in good accordance with the same phenolic composite formulations regarding phenolic and polybenzoxazine polymers have densities that are very close. [16] When the theoretical densities that are calculated according to the predetermined density and weight percentages of the constituents are compared to experimental densities, it is seen that the experimental density is in good accordance with the theoretical values. Therefore, one can conclude that the amount of the porosity inside the composites, if there is any, is not significant, and the benzoxazine resin filled the gaps in the composites well. The existence of significant porosity could not be determined in the scanning electron micrographs either.

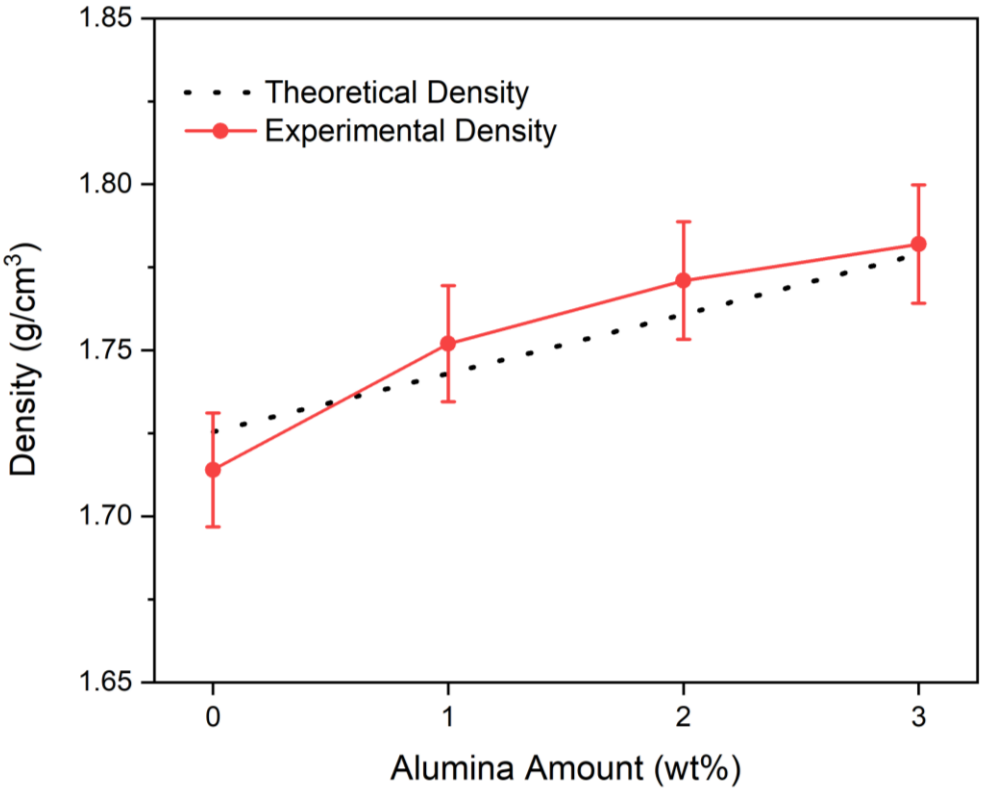

Figure 4.9 Experimental density values of the polybenzoxazine composites

4.2.1 Mechanical Properties of the Polybenzoxazine Composites

The promising candidates to be used in the thermal protection systems of high-performance systems, such as in aerospace applications, must have great mechanical properties especially shear strength because the insulations in thrust systems mostly expose to shear stresses during operation. The flexural strength (Figure 4.10.a) and the interlaminar shear strength tests (Figure 4.10.b) were conducted on at least five specimens following the standards.

Three-point bending tests were performed on the composite samples to determine the flexural strengths of the composites, and the results are presented in Figure 4.11. While the neat polybenzoxazine composite has 160.56 ± 13.40 MPa of flexural strength, only 1 wt% alumina containing polybenzoxazine composite reached a flexural strength of 173.00 ± 16.84 MPa which means more than 7% increase in the flexural strength. 2 wt% alumina containing polybenzoxazine composites have reached 174.42 ± 3.84 MPa of flexural strength while maintaining the increase trend. The final composite, named as PBZ3, with 3 wt% alumina possesses 178.60 ± 6.70 MPa flexural strength which is 11% higher than the neat polybenzoxazine composite.

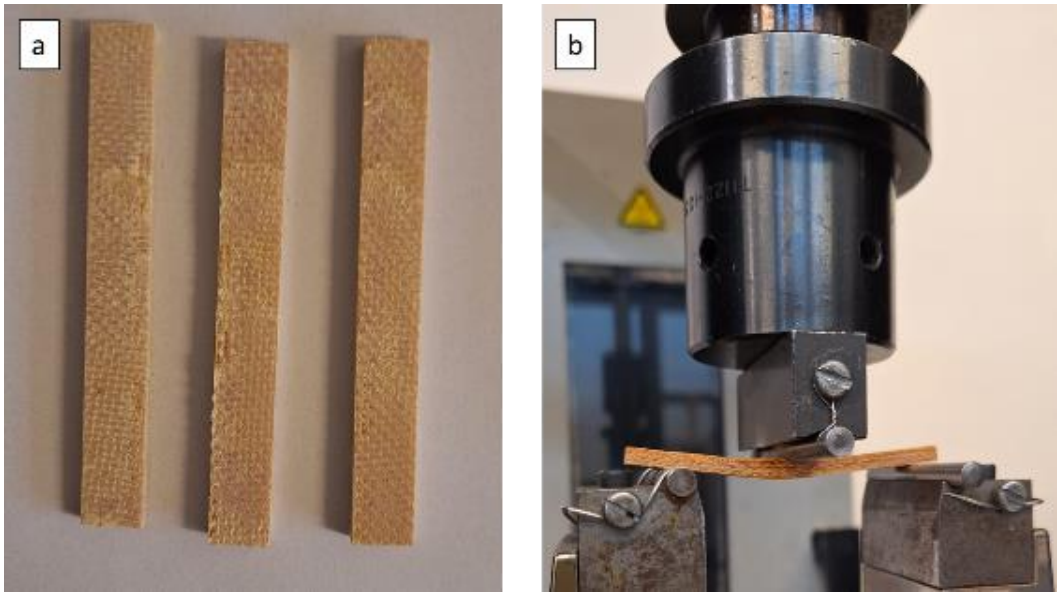

Figure 4.10 a) Flexural strength test samples b) Three point bending test

The interlaminar shear strength (ILSS) tests were employed to examine how well the laminates of polybenzoxazine composites adhere to each other. For this purpose, samples were exposed to shear forces till the break point, that is the point at which the laminates are split off. The higher the adherence between the laminates, the higher the interlaminar shear strength values should be. As given in Figure 4.11, the neat polybenzoxazine composites have an interlaminar shear strength of only 9.18 ± 0.5 MPa. Adding 1 wt% alumina caused the composite to have 10.04 ± 1.03 MPa of interlaminar shear strength. 2 wt% alumina caused a higher ILSS value which is 11.15 ± 0.65, and the 3 wt% alumina containing composites have 11.63 ± 0.61 MPa of ILSS value, corresponding to a total of about 27% increase. The trend of ILSS values increasing with increasing alumina particles in the structure is proportional. These results imply that the interaction between alumina particles and polybenzoxazine resin is strong. The reason why ILSS values increase with the addition of alumina particles can be attributed to alumina particles acting as a physical barrier between the laminates causing them to separate harder when they are exposed to shear forces.

Overall, it is observed that the addition of alumina particles improves both the flexural and the interlaminar shear strengths of the silica fiber-reinforced polybenzoxazine composites which are beneficial regarding the required mechanical strength of ablative composites used in thermal protection systems that work under extremely harsh environments.

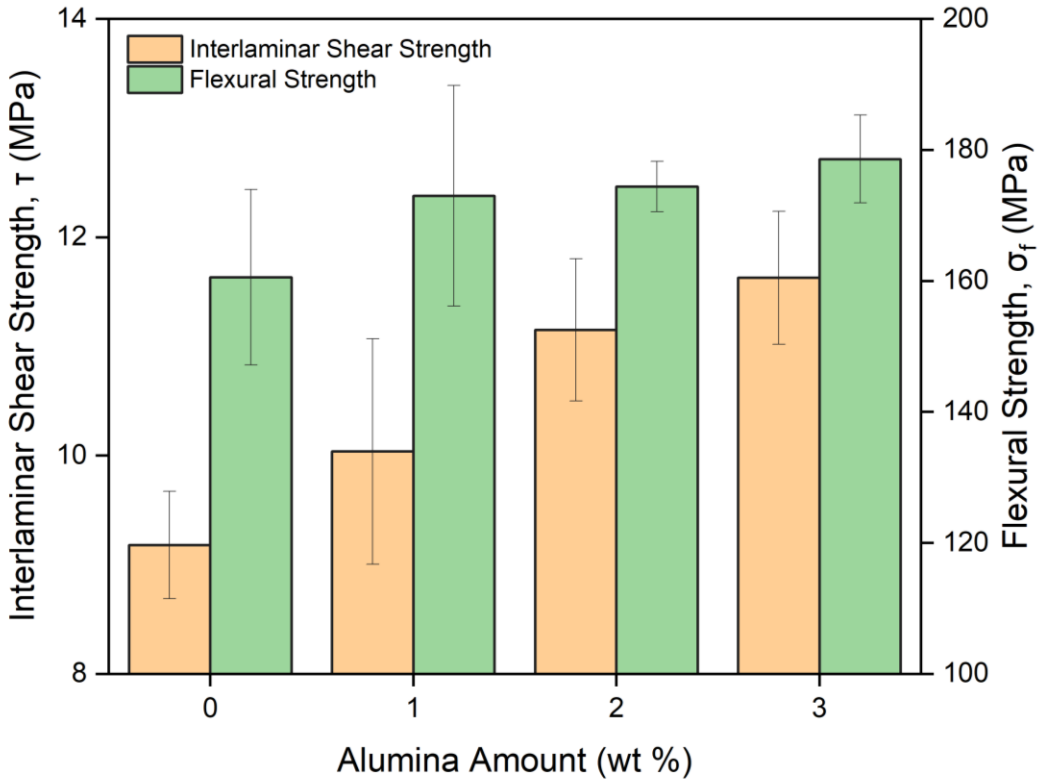

Figure 4.11 The influence of alumina addition into the silica fiber-reinforced polybenzoxazine composites on the mechanical properties.

4.2.2 Thermal Properties of Polybenzoxazine Composites

The most important and vital feature of a material aimed at being used in the thermal protection systems of aerospace industry as ablative material is its thermal properties. The thermal characteristics of the material like ablation performance and thermal stability determine the quality and usability of that material.

The ablation performances of the polybenzoxazine composites were determined by the oxyacetylene ablation test. This test was conducted on oxyacetylene test samples which are machined into 30 mm diameter disks with 10 mm thickness (shown in Figure 4.12) using the oxyacetylene ablation test equipment (shown in Figure 4.13) according to GJB323A-96. The oxyacetylene ablation test is conducted in three

steps. First, the mass of the oxyacetylene test samples is measured. Secondly, the oxyacetylene test samples are exposed to an extremely high temperature oxyacetylene flame with a heat flux of 4200 kW/m^2 for 20 seconds, and the temperature of this flame reaches 3000 °C. Thirdly and finally, the mass of the oxyacetylene test samples exposed to the flame is measured again, and the difference is divided by the test duration. The mass ablation rates of the polybenzoxazine composites are compared in Figure 4.14. The neat polybenzoxazine composite had a mass ablation rate of 0.0334 ± 0.0022 g/s, whereas 1 wt% alumina particle containing composite had 0.0329 ± 0.0007 g/s. This trend continued with 2 and 3 wt% alumina particle-containing composites giving 0.0323 ± 0.0007 and 0.0284 ± 0.0006 g/s ablation rates, respectively. This means that adding 1 and 2 wt% alumina to the polybenzoxazine composite reduced the ablation rate by only 1.35% and %3.41, the 3 wt% alumina addition caused a much more significant decrease, 14.87%, in the mass ablation rate when compared to neat polybenzoxazine composite. This increased ablative performance gives a chance to the design of aerospace systems with thinner insulation materials, allowing an increased amount of propellant inside which causes higher range and flying time for the aerospace vehicle.

Yet, the reports in the literature showed that additions of nano-Al_2O_3 on vitreous silica fiber-reinforced phenolic composites [55] or o-MMT nano-clay on the properties of carbon fiber-reinforced polybenzoxazine composite [56] adversely affects the ablative properties. However, as compared in Figure 4.15, the mass ablation rates of the submicron alumina-filled silica fiber-reinforced polybenzoxazine composites produced in this study are much lower compared to many other studies reported on the ablative composites in the literature, including other phenolic composites [57-60], cyanate ester composite [61], bismaleimide composite [62], EPDM rubber [63-65], silicone rubber [66-68], and other polybenzoxazine composites [14], [69].

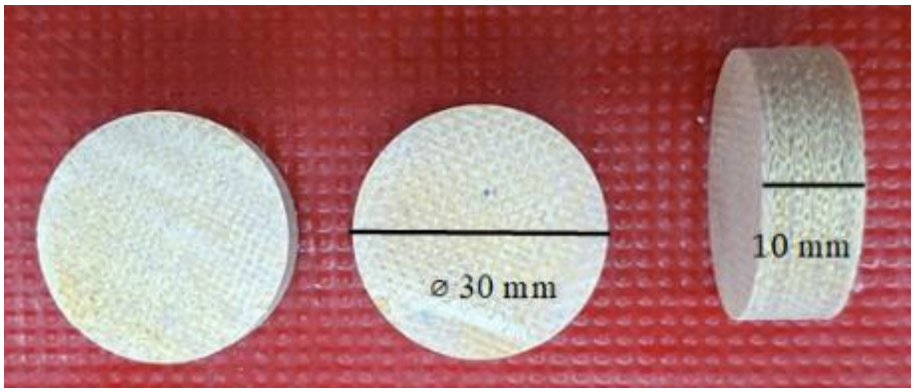

Figure 4.12 Oxyacetylene test samples according to GJB323A-96 standard

Figure 4.13 Oxyacetylene test equipment during ablation testing

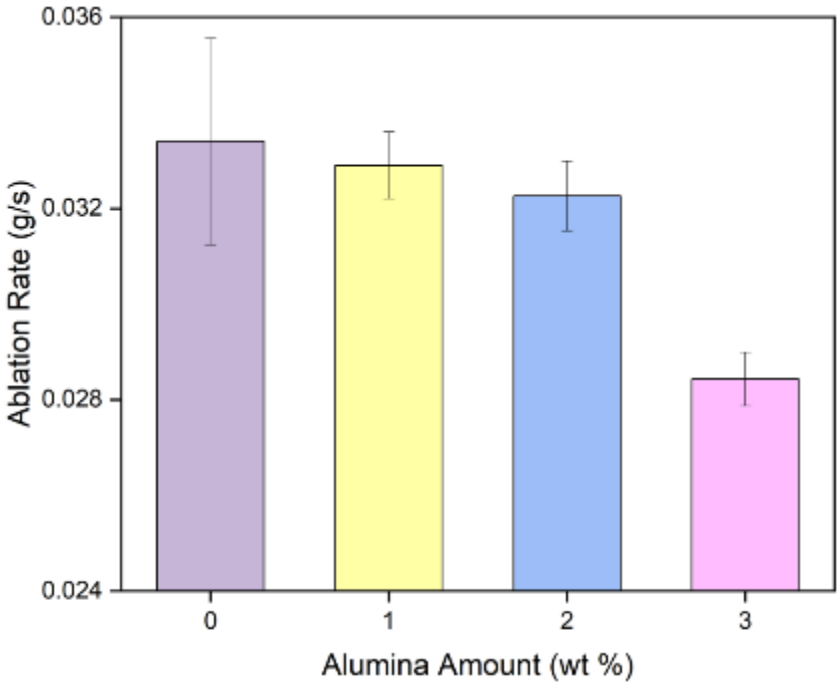

Figure 4.14 Mass ablation rate of polybenzoxazine composites (PBZ0, PBZ1, PBZ2, and PBZ3)

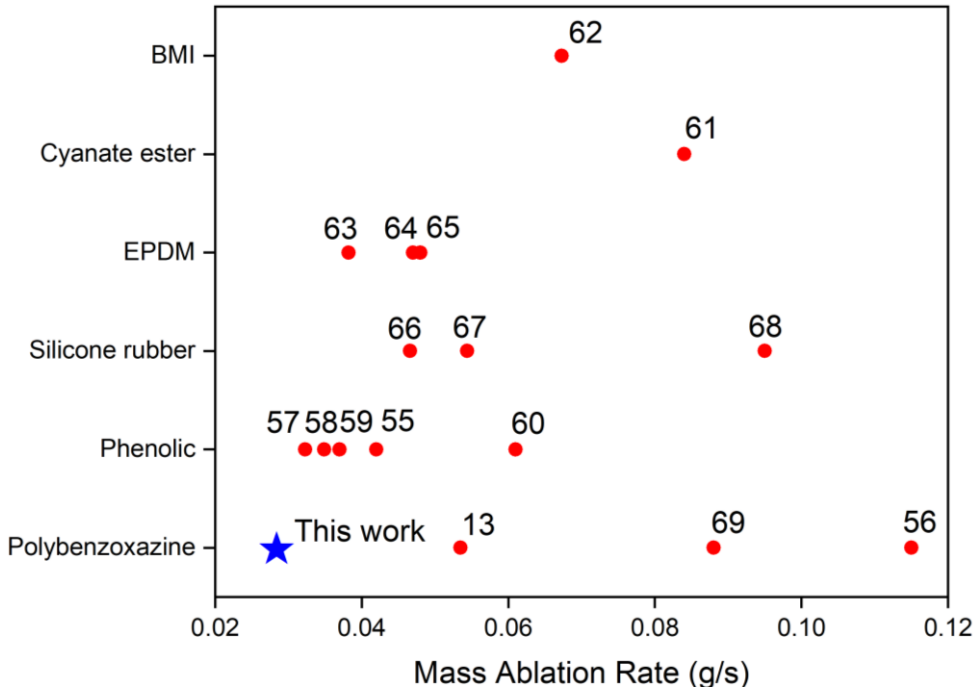

Figure 4.15 Comparison of mass ablation rates of polybenzoxazine composites with other studies from literature

Then, X-ray diffraction analysis was employed on the ablated composites to reveal the ablation mechanism and chemical reactions occurred during ablation. As shown in the comparison of PBZ0 and PBZ3 samples in Figure 4.16, after being exposed to oxyacetylene flame for a long period, the char (carbonaceous layer) formed on the composites' surface. The presence of both graphitized and amorphous carbon is evident from the broad peak at 27° [70] and at 44° [14], respectively, in the diffractograms, formed due to pyrolysis of polybenzoxazine, a carbon-rich polymer, with ablation. PBZ3 also shows sharp peaks at angles of 37.16, 39.72, 45.30, 54.42, 59.42, 68.28, 70.02, and 78.60. These peaks were assigned to alumina particles in the structure; however, they all shifted approximately 2° to higher angle values when compared to the XRD pattern of the alumina particles before the ablation test (provided in Fig 3, JCPDS reference pattern no: 46-1212). The shift of the peaks may be attributed to the reduction in the lattice spacing caused by the stress exerted on them by the matrix material. Lastly, a small amount of SiC formation during the exposure to oxyacetylene flame was depicted in the diffractograms. The small peaks observed near 61.82° and 73.28° were assigned to SiC, which was formed during the oxyacetylene test by the possible reactions of [1] and [2] between silica fibers and pyrolyzed carbon at extremely high temperatures of the test. [14] [58]

$$SiO_{2(s)} + 3C_{(s)} \rightarrow SiC_{(s)} + 2CO_{(g)} \quad [1]$$

$$SiO_{2(s)} + 2C_{(s)} \rightarrow SiC_{(s)} + CO_{2(g)} \quad [2]$$

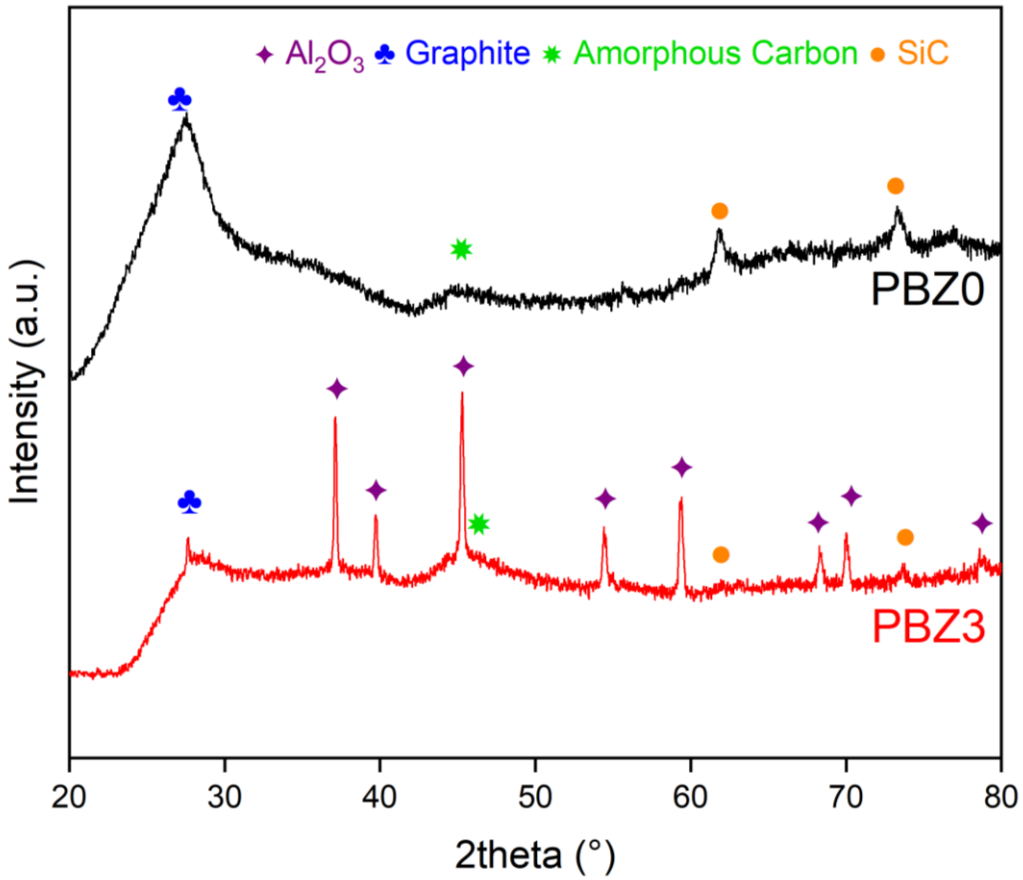

Figure 4.16 X-ray diffractogram of the ablated composites (PBZ0 and PBZ3)

To further investigate the ablation mechanism, the surface morphologies of the composite samples are analyzed via SEM micrographs. As given in Figure 4.17 the surface morphology of the polybenzoxazine composites has altered after the exposure to oxyacetylene flame when compared to unexposed images given in Figure 4.3 and Figure 4.4. The ablated surfaces of the four different composites exhibit molten glassy droplets which are formed by the melting of the silica fibers due to the extremely high temperature of the oxyacetylene test. It is thought that because of the high surface energy, the molten silica droplets could not extend on the surface of the carbon layer created due to the pyrolyzed polybenzoxazine.[14] This melting process, which is an endothermic reaction, absorbs lots of the energy present in the oxyacetylene flame and hinders the degradation of the composites, and

provides a heat barrier. The distribution of the alumina particles in composites after oxyacetylene ablation test can be examined in the elemental mapping image of PBZ3 which is given in Figure 4.18 as it shows that alumina particles are dispersed throughout the structure homogenously even after ablation. The composites that contain alumina particles resulted in better ablation performances in proportion to the alumina amount as explained in Figure 4.14, and the possible reason for that can be the barrier effect of the alumina particles that prevent the passage of the oxyacetylene flame into the inside of the composites. When the high temperature flame cannot pass through the inside of the composite structure, it results in less of the mass of the composite system to form char layer. This situation directly reduces the mass ablation rate. Other suggestion to the better performance of alumina containing composites can be the increase in the mechanical strength of the char, due to inorganic alumina particle incorporation with strong interfacial bonding between the polybenzoxazine, silica fibers and alumina particles, which makes the char to break harder which leads it to stick to the composite more and this results in lower mass ablation rate.

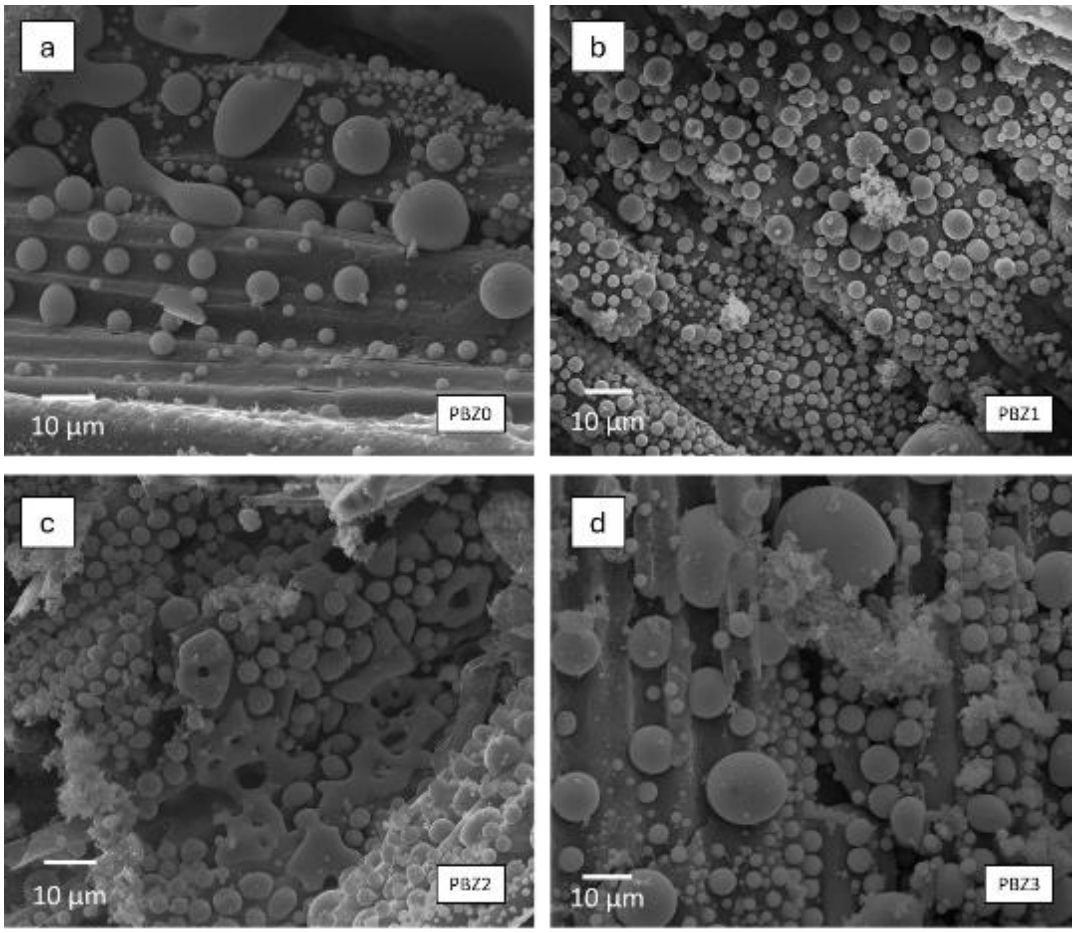

Figure 4.17 The surface morphology of the polybenzoxazine composites after oxyacetylene ablation test

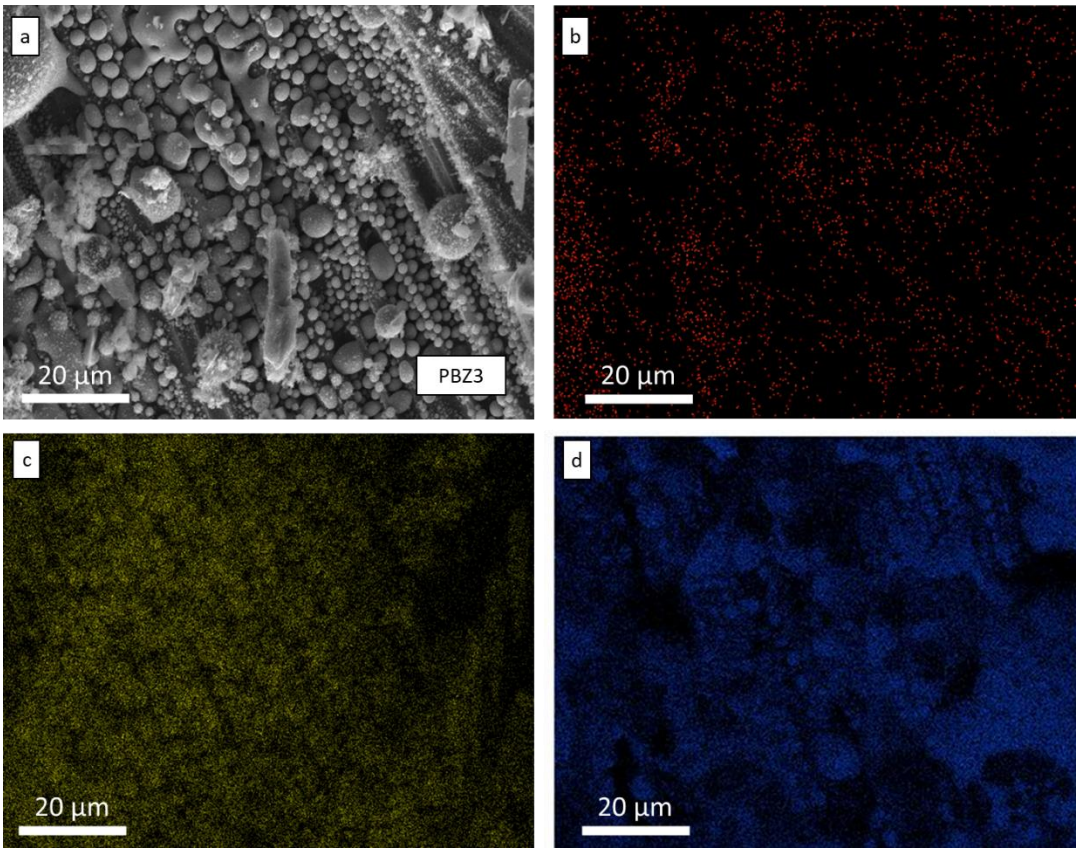

Figure 4.18 Elemental mapping image of PBZ3 after oxyacetylene ablation test

To examine the effect of combining silica fiber and alumina particles with polybenzoxazine on thermal stability, thermogravimetric analysis is conducted as mentioned before, and the TGA and DTG curves can be examined together in Figure 4.19. The residual mass percentage of pristine polybenzoxazine at 900 °C 33.56 % of the initial mass. When polybenzoxazine was reinforced with silica fiber neat and creates the composite PBZ0, the residual mass percentage rises to 78.17% at 800 °C. These are already expected, because PBZ0 is formed with 67 wt% of silica fibers, and silica is known to be extremely thermally stable, and it postponed the degradation of polybenzoxazine by increasing the thermal stability of the overall composite. When 1 wt% alumina particles are introduced to the system, the residual mass percentage does not alter significantly, it nearly stays the same. In our study, when the alumina particle amount in the composite is increased to 2 wt%, the

residual mass at 900 °C increases to 79.10%. Addition of 3 wt% alumina particle causes a notable increase to the residual mass at 900 °C of polybenzoxazine composite, it becomes 81.10%. These results mean that the addition of alumina particles causes the polybenzoxazine composite to yield more material at high temperatures, however it is important to note that the degradation rate becomes higher at the degradation onset temperatures with alumina particle incorporation as is reported in the DTG curve presented in Figure 4.19. Also, the alumina particle incorporation into the structure alters the degradation temperatures when compared to neat polybenzoxazine composite (PBZ0) and polybenzoxazine polymer. A similar situation was also observed in the study of Z. Lule et al. in which they created PLA-Alumina composites. They observed that the addition of alumina particles causes the PLA to degrade earlier, and faster, however alumina added composites yielded more material at the end of the test like our study. [71] These data show that alumina addition performs as a heat shielding material and causes the polybenzoxazine composites to be more thermally stable, protecting the overall composite by absorbing the excessive heat, which is similarly seen in our ablation test and in other studies.[72] [73]

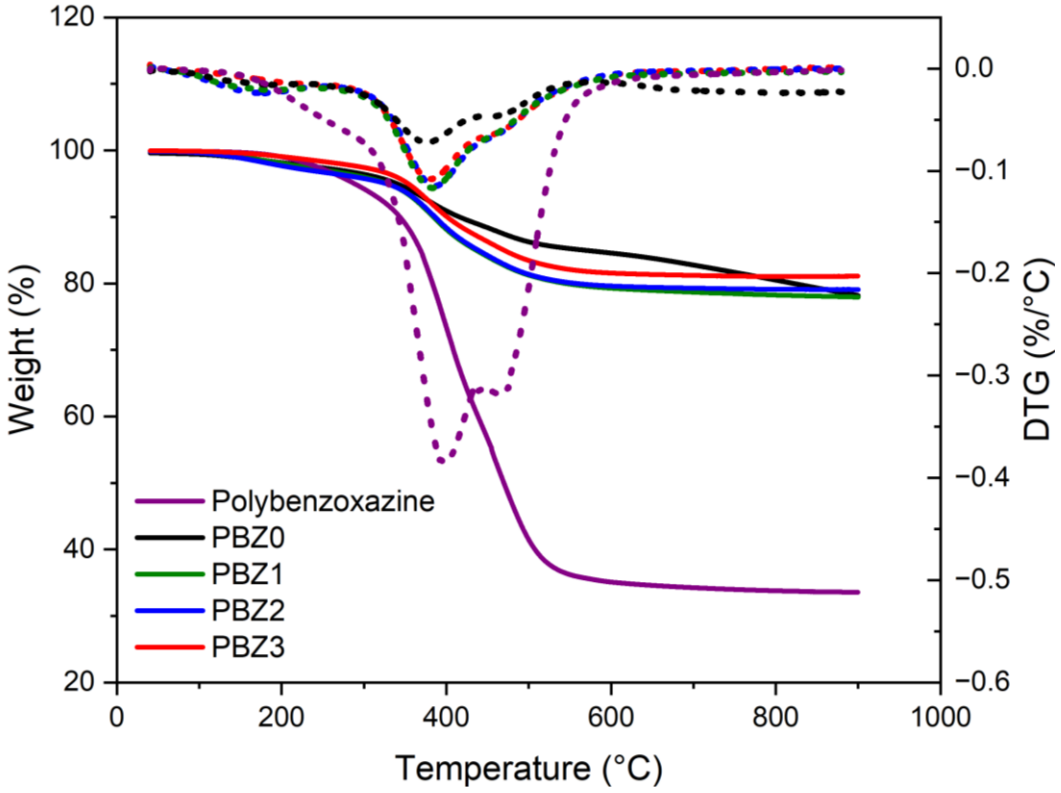

Figure 4.19 Thermogravimetric and derivative thermogravimetric curves of polybenzoxazine and polybenzoxazine composites

In addition to mass ablation performance and thermal stability, the effect of alumina particle introduction on thermal diffusivity values of the polybenzoxazine composites were also examined in this study because it tells how the temperature transfer will be affected. In this research, it is seen in Figure 4.20 that the addition of alumina particles increases the thermal diffusivity of the material. For the composites, the thermal diffusivities at 25 °C were found to be 0.00317, 0.00370, 0.00373, and 0.00407 cm^2/s for PBZ0, PBZ1, PBZ2, and PBZ3 respectively. However, there is an incompatibility between the thermal diffusivity values of PBZ1 and PBZ2 after 50 °C. At the end of the test at 175 °C, the thermal diffusivity values became 0.00237, 0.00283, 0.00280, and 0.00283 cm^2/s for the composites. The incompatibility, which can be seen in Figure 4.19, of PBZ1 and PBZ2 can be attributed to the possible agglomeration of alumina particles in the composite PBZ2.

Similar research was followed by Y. Ouyang et al, they have studied the effect of alumina addition on the thermal diffusivity and conductivity of the phenolic resin. They have stated that neat phenolic resin had a thermal diffusivity of 0.00134 cm^2/s, and the composite with 50 wt% branched Al_2O_3 had 0.00308 cm^2/s of thermal diffusivity. When the alumina content rises to 75 wt%, the thermal diffusivity value becomes 0.00598 cm^2/s. [74] Another study regarding thermal diffusivity was conducted by Plengudomkit et al. They have added graphene into benzoxazine. They have demonstrated that the addition of graphene to benzoxazine causes the thermal diffusivity values to increase. For example, at 25°C they measure the thermal diffusivity of polybenzoxazine as 0.0131 cm^2/s. Adding 10 wt% graphene to the structure causes the thermal diffusivity to increase to 0.0509 cm^2/s and adding 60 wt% graphene to the structure causes the value to become 0.4861 cm^2/s. [75] Also, it is examined in our study that when the temperature is increased, the thermal diffusivity values of our polybenzoxazine composites decrease. The decrease in thermal diffusivity with increased temperature is expected, and this drop is also seen in similar articles dealing with polymer composites. [76-78] The decrease of thermal diffusivity with increased temperature is attributed to increased phonon-phonon scattering with increased temperature, which at the end reduces the thermal diffusivity values. [79]

Also, the thermal conductivity values of the polybenzoxazine composites are calculated according to Equation 2 where K is the thermal conductivity (W/m.K), α is thermal diffusivity (cm^2/s), ρ is the density (g/cm^3), and C_p is the specific heat capacity (J/(kg.K)). The C_p is determined according to a DSC analysis performed with well-characterized reference material which was sapphire, ρ is already measured, and α is calculated with TA Instruments DLF 1600.

$$K = \alpha * \rho * C_p \qquad [2]$$

The thermal conductivity values of polybenzoxazine composites after calculations are given in Figure 4.20. It is seen that PBZ0 has a thermal conductivity value of 0.4841 W/m.K at 25 °C, addition of 1 wt% alumina caused an increase in the thermal conductivity to reach 0.5246 W/m.K. PBZ2 and PBZ3 had thermal conductivity values of 0.5116 and 0.4090 W/m.K. Addition of alumina first increased the thermal conductivity of neat polybenzoxazine composite, then the trend reverses and the thermal conductivity values starts to decrease with increased alumina content. Similar situations are also seen at higher temperatures. Alumina particles generally enhance the thermal conductivity because of their high intrinsic thermal conductivity. However, poor dispersion of alumina particles in the polymer matrix can hinder the efficient thermal conduction pathways, potentially decreasing overall thermal conductivity. The thermal conductivity values can decrease if alumina particles start to form agglomerates which then acts as thermal barriers. Also, addition of alumina particles may disrupt the thermal conduction pathways of silica fibers, thus reducing the overall thermal conductivity of the composite.

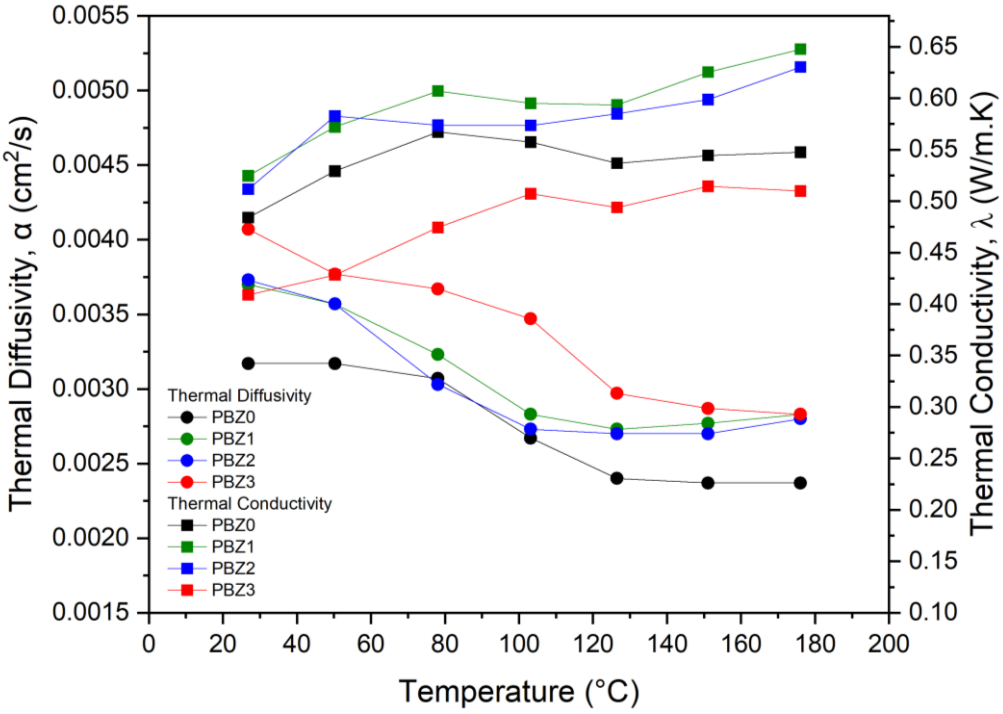

Figure 4.20 Thermal diffusivity curve of polybenzoxazine composites

CHAPTER 5

CONCLUSIONS

This research displays the successful production of novel silica fiber-reinforced polybenzoxazine composites filled with submicron alumina particles (0, 1, 2, 3 wt%), and characterization of their mechanical and thermal properties with main main focus of the influence of submicron alumina particle incorporation to the silica fiber-reinforced polybenzoxazine composites' ablation performance and ablation mechanism.

It is found that submicron alumina particle incorporation increases the mechanical properties of polybenzoxazine composites, and results in better ablative properties. The flexural strength and interlaminar shear strength values were increased from 160.56 and 9.18 MPa to 178.60 and 11.63 MPa, respectively, when 3 wt.% alumina particles were added into the neat polybenzoxazine composite.

The ablative properties regarding the mass ablation rate of the polybenzoxazine composites improved 15% by adding only 3 wt% alumina by reducing the mass ablation rate from 0.0334 to 0.0284 g/s. This mass ablation rate value is one of the lowest in the literature among the oxyacetylene test results of ablative composites including phenolic composites. This very small ablation rate means that alumina filled polybenzoxazine composites will perform better than many commonly used ablative materials. The increased ablation performance of alumina added polybenzoxazine composites allow the design of thermal protection systems with thinner ablative insulations leaving more volume for the propellant, which directly causes increased range and speed for rockets and missiles. Moreover, the thermal durability of the polybenzoxazine composites boosted with the addition of alumina. The residual mass at 900 °C was found to be 81.10% for 3 wt% alumina containing composite, while the neat composite has only 78.17%. Other than oxyacetylene and

thermogravimetric analysis, the effect of alumina particles on thermal diffusivity of the polybenzoxazine composites was reported. The overall thermal characterization of the polybenzoxazine composites suggests that these materials are appropriate for usage in thermal protection systems in the aerospace industry.

This thesis study showed that polybenzoxazine based composite materials are promising and compelling candidates to be used for ablative components in aerospace industry, and their intrinsic excellent properties are demonstrated to be further enhanced by addition of alumina particles to the structure, making them more favorable for the usage in ablative thermal protection systems instead of toxic phenolic materials which is aimed to be removed from the aerospace and other industries.

REFERENCES

[1] M. R. Kessler, “Polymer Matrix Composites: A Perspective for a Special Issue of Polymer Reviews,” Polymer Reviews, vol. 52, no. 3. Informa UK Limited, pp. 229–233, Jul. 2012. doi: 10.1080/15583724.2012.708004.

[2] T. Sathishkumar, S. Satheeshkumar, and J. Naveen, “Glass fiber-reinforced polymer composites – a review,” Journal of Reinforced Plastics and Composites, vol. 33, no. 13. SAGE Publications, pp. 1258–1275, Apr. 08, 2014. doi: 10.1177/0731684414530790.

[3] S. Kangishwar, N. Radhika, A. A. Sheik, A. Chavali, and S. Hariharan, “A comprehensive review on polymer matrix composites: material selection, fabrication, and application,” Polymer Bulletin, vol. 80, no. 1. Springer Science and Business Media LLC, pp. 47–87, Jan. 23, 2022. doi: 10.1007/s00289-022-04087-4.

[4] P. Robinson, E. S. Greenhalgh, and S. Pinho, Failure Mechanisms in Polymer Matrix Composites: Criteria, Testing and Industrial Applications. Cambridge, UK: Woodhead Publishing, 2012.

[5] J. M. Sands, B. K. Fink, S. H. McKnight, C. H. Newton, J. W. Gillespie Jr., and G. R. Palmese, “Environmental issues for polymer matrix composites and structural adhesives,” Clean Products and Processes, vol. 2, no. 4. Springer Science and Business Media LLC, pp. 0228–0235, Feb. 07, 2001. doi: 10.1007/s100980000089.

[6] M. Natali, J. M. Kenny, and L. Torre, “Science and technology of polymeric ablative materials for thermal protection systems and propulsion devices: A review,” Progress in Materials Science, vol. 84. Elsevier BV, pp. 192–275, Dec. 2016. doi: 10.1016/j.pmatsci.2016.08.003.

[7] H. J. ALLEN, “Hypersonic Flight and the Re-Entry Problem: The Twenty-First Wright Brothers Lecture,” Journal of the Aerospace Sciences, vol. 25, no. 4.

American Institute of Aeronautics and Astronautics (AIAA), pp. 217–227, Apr. 1958. doi: 10.2514/8.7600.

[8] C. V. Kumar and B. Kandasubramanian, “Advances in Ablative Composites of Carbon Based Materials: A Review,” Industrial & Engineering Chemistry Research, vol. 58, no. 51. American Chemical Society (ACS), pp. 22663–22701, Nov. 26, 2019. doi: 10.1021/acs.iecr.9b04625.

[9] T. Brown and P. Pitfield, “Tungsten,” Critical Metals Handbook. Wiley, pp. 385–413, Dec. 27, 2013. doi: 10.1002/9781118755341.ch16.

[10] A. I. Savvatimskiy, “Measurements of the melting point of graphite and the properties of liquid carbon (a review for 1963–2003),” Carbon, vol. 43, no. 6. Elsevier BV, pp. 1115–1142, May 2005. doi: 10.1016/j.carbon.2004.12.027.

[11] Zazula, Jan M. On graphite transformations at high temperature and pressure induced by absorption of the LHC beam. No. LHC-Project-Note-78. CERN-LHCProject-Note-78, 1997.

[12] T. Takeichi, T. Kawauchi, and T. Agag, “High Performance Polybenzoxazines as a Novel Type of Phenolic Resin,” Polymer Journal, vol. 40, no. 12. Springer Science and Business Media LLC, pp. 1121–1131, Jun. 25, 2008. doi: 10.1295/polymj.pj2008072.

[13] K. George, B. P. Panda, S. Mohanty, and S. K. Nayak, “Recent developments in elastomeric heat shielding materials for solid rocket motor casing application for future perspective,” Polymers for Advanced Technologies, vol. 29, no. 1. Wiley, pp. 8–21, Jul. 12, 2017. doi: 10.1002/pat.4101.

[14] Z. Deng, Y. Lv, M. Shi, Z. Huang, and W. Huang, “A Novel Fused SiO2 and h-BN Modified Quartz Fiber/Benzoxazine Resin Ceramizable Composite with Excellent Flexural Strength and Ablation Resistance,” Polymers, vol. 15, no. 22. MDPI AG, p. 4430, Nov. 16, 2023. doi: 10.3390/polym15224430.

[15] N. N. Ghosh, B. Kiskan, and Y. Yagci, “Polybenzoxazines—New high performance thermosetting resins: Synthesis and properties,” Progress in Polymer Science, vol. 32, no. 11. Elsevier BV, pp. 1344–1391, Nov. 2007. doi: 10.1016/j.progpolymsci.2007.07.002.

[16] H. Ishida and D. J. Allen, “Physical and mechanical characterization of near-zero shrinkage polybenzoxazines,” Journal of Polymer Science Part B: Polymer Physics, vol. 34, no. 6. Wiley, pp. 1019–1030, Apr. 30, 1996. doi: 10.1002/(sici)1099-0488(19960430)34:6<1019::aid-polb1>3.0.co;2-t.

[17] B. Kiskan, N. N. Ghosh, and Y. Yagci, “Polybenzoxazine-based composites as high-performance materials,” Polymer International, vol. 60, no. 2. Wiley, pp. 167–177, Oct. 28, 2010. doi: 10.1002/pi.2961.

[18] F. W. Holly and A. C. Cope, “Condensation Products of Aldehydes and Ketones with o-Aminobenzyl Alcohol and o-Hydroxybenzylamine,” Journal of the American Chemical Society, vol. 66, no. 11. American Chemical Society (ACS), pp. 1875–1879, Nov. 1944. doi: 10.1021/ja01239a022.

[19] P. Mora, M. Okhawilai, C. Jubsilp, C. W. Bielawski, and S. Rimdusit, “Glass fabric reinforced polybenzoxazine composites filled with nanosilica: A High impact response poises use as strike panels in multilayered armor applications,” Journal of Materials Research and Technology, vol. 9, no. 6. Elsevier BV, pp. 12723–12736, Nov. 2020. doi: 10.1016/j.jmrt.2020.09.005.

[20] L. Dumas, L. Bonnaud, M. Olivier, M. Poorteman, and P. Dubois, “Multiscale benzoxazine composites: The role of pristine CNTs as efficient reinforcing agents for high-performance applications,” Composites Part B: Engineering, vol. 112. Elsevier BV, pp. 57–65, Mar. 2017. doi: 10.1016/j.compositesb.2016.12.039.

[21] A. H. Telli, “Preparation and characterization of polybenzoxazine involving various additives,” thesis, Middle East Technical University, Ankara, 2021

[22] T. Takeichi, Y. Guo, and T. Agag, “Synthesis and characterization of poly(urethane-benzoxazine) films as novel type of polyurethane/phenolic resin

composites," Journal of Polymer Science Part A: Polymer Chemistry, vol. 38, no. 22. Wiley, pp. 4165–4176, 2000. doi: 10.1002/1099-0518(20001115)38:22<4165::aid-pola170>3.0.co;2-s.

[23] T. Lakshmikandhan, A. Chandramohan, K. Sethuraman, and M. Alagar, "Development and characterization of functionalized Al2O3and TiO2-reinforced polybenzoxazine nanocomposites," Designed Monomers and Polymers, vol. 19, no. 1. Informa UK Limited, pp. 67–76, Oct. 13, 2015. doi: 10.1080/15685551.2015.1092014.

[24] Q. Chen, R. Xu, and D. Yu, "Multiwalled carbon nanotube/polybenzoxazine nanocomposites: Preparation, characterization and properties," Polymer, vol. 47, no. 22. Elsevier BV, pp. 7711–7719, Oct. 2006. doi: 10.1016/j.polymer.2006.08.058.

[25] H. Ishida and H. Y. Low, "Synthesis of benzoxazine functional silane and adhesion properties of glass-fiber-reinforced polybenzoxazine composites," Journal of Applied Polymer Science, vol. 69, no. 13. Wiley, pp. 2559–2567, Sep. 26, 1998. doi: 10.1002/(sici)1097-4628(19980926)69:13<2559::aid-app5>3.0.co;2-9.

[26] C. A. Wilkie and A. B. Morgan, Fire Retardancy of Polymeric Materials, Second Edition. CRC Press, 2009.

[27] S. Boryniec and W. Przygocki, "Polymer Combustion Processes. 3. Flame Retardants for Polymeric Materials," Progress in Rubber and Plastics Technology, vol. 17, no. 2. SAGE Publications, pp. 127–148, May 2001. doi: 10.1177/147776060101700204.

[28] G. Camino, L. Costa, and M. P. Luda di Cortemiglia, "Overview of fire retardant mechanisms," Polymer Degradation and Stability, vol. 33, no. 2. Elsevier BV, pp. 131–154, Jan. 1991. doi: 10.1016/0141-3910(91)90014-i.

[29] M Le Bras and R. Society, Fire retardancy of polymers : new applications of mineral fillers. Cambridge, Uk: Royal Society Of Chemistry, 2005.

[30] L. Chen and Y. Wang, “A review on flame retardant technology in China. Part I: development of flame retardants,” Polymers for Advanced Technologies, vol. 21, no. 1. Wiley, pp. 1–26, Sep. 22, 2009. doi: 10.1002/pat.1550.

[31] G. Camino, A. Maffezzoli, M. Braglia, M. De Lazzaro, and M. Zammarano, “Effect of hydroxides and hydroxycarbonate structure on fire retardant effectiveness and mechanical properties in ethylene-vinyl acetate copolymer,” Polymer Degradation and Stability, vol. 74, no. 3. Elsevier BV, pp. 457–464, Jan. 2001. doi: 10.1016/s0141-3910(01)00167-7.

[32] M. M. Velencoso, A. Battig, J. C. Markwart, B. Schartel, and F. R. Wurm, “Molecular Firefighting—How Modern Phosphorus Chemistry Can Help Solve the Challenge of Flame Retardancy,” Angewandte Chemie International Edition, vol. 57, no. 33. Wiley, pp. 10450–10467, Jun. 29, 2018. doi: 10.1002/anie.201711735.

[33] S. V. Levchik, G. F. Levchik, A. I. Balabanovich, G. Camino, and L. Costa, “Mechanistic study of combustion performance and thermal decomposition behaviour of nylon 6 with added halogen-free fire retardants,” Polymer Degradation and Stability, vol. 54, no. 2–3. Elsevier BV, pp. 217–222, Nov. 1996. doi: 10.1016/s0141-3910(96)00046-8.

[34] U. Braun and B. Schartel, “Flame Retardant Mechanisms of Red Phosphorus and Magnesium Hydroxide in High Impact Polystyrene,” Macromolecular Chemistry and Physics, vol. 205, no. 16. Wiley, pp. 2185–2196, Oct. 26, 2004. doi: 10.1002/macp.200400255.

[35] B. Liu, H. Zhao, and Y. Wang, “Advanced Flame-Retardant Methods for Polymeric Materials,” Advanced Materials, vol. 34, no. 46. Wiley, Feb. 27, 2022. doi: 10.1002/adma.202107905.

[36] S.-Y. Lu and I. Hamerton, “Recent developments in the chemistry of halogen-free flame retardant polymers,” Progress in Polymer Science, vol. 27, no. 8. Elsevier BV, pp. 1661–1712, Oct. 2002. doi: 10.1016/s0079-6700(02)00018-7.

[37] L. D. Hart, Alumina chemicals : science and technology handbook. Westerville, Ohio: American Ceramic Society, 1990.

[38] I. Levin and D. Brandon, “Metastable Alumina Polymorphs: Crystal Structures and Transition Sequences,” Journal of the American Ceramic Society, vol. 81, no. 8. Wiley, pp. 1995–2012, Aug. 1998. doi: 10.1111/j.1151-2916.1998.tb02581.x.

[39] G. Paglia, “Determination of the structure of Y-alumina using empirical and first principle calculations combined with supporting experiments,” thesis, Curtin University, Perth, 2004

[40] N. M. Stuart and K. Sohlberg, “The Microstructure of γ-Alumina,” Energies, vol. 14, no. 20. MDPI AG, p. 6472, Oct. 10, 2021. doi: 10.3390/en14206472.

[41] A. M. Abyzov, “Aluminum Oxide and Alumina Ceramics (review). Part 1. Properties of Al2O3 and Commercial Production of Dispersed Al2O3,” Refractories and Industrial Ceramics, vol. 60, no. 1. Springer Science and Business Media LLC, pp. 24–32, May 15, 2019. doi: 10.1007/s11148-019-00304-2.

[42] L. Paglia et al., “Manufacturing, thermochemical characterization and ablative performance evaluation of carbon-phenolic ablative material with nano-Al2O3 addition,” Polymer Degradation and Stability, vol. 169. Elsevier BV, p. 108979, Nov. 2019. doi: 10.1016/j.polymdegradstab.2019.108979.

[43] B. Wetzel, F. Haupert, and M. Qiu Zhang, “Epoxy nanocomposites with high mechanical and tribological performance,” Composites Science and Technology, vol. 63, no. 14. Elsevier BV, pp. 2055–2067, Nov. 2003. doi: 10.1016/s0266-3538(03)00115-5.

[44] S. Ali et al., “Microstructural and thermal analysis of alumina modified carbon/phenolic composites after ablation testing,” Journal of Composite Materials, vol. 57, no. 5. SAGE Publications, pp. 885–896, Dec. 20, 2022. doi: 10.1177/00219983221147389.

[45] J. Kajornchaiyakul, C. Jubsilp, and S. Rimdusit, “Thermal and Mechanical Properties of Highly-Filled Polybenzoxazine-Alumina Composites,” Key Engineering Materials, vol. 545. Trans Tech Publications, Ltd., pp. 211–215, Mar. 2013. doi: 10.4028/www.scientific.net/kem.545.211.

[46] H. Liu, G. Ning, Z. Gan, and Y. Lin, “Emulsion-based synthesis of unaggregated, spherical alpha alumina,” Materials Letters, vol. 62, no. 10–11. Elsevier BV, pp. 1685–1688, Apr. 2008. doi: 10.1016/j.matlet.2007.09.059.

[47] F. R. Feret, D. Roy, and C. Boulanger, “Determination of alpha and beta alumina in ceramic alumina by X-ray diffraction,” Spectrochimica Acta Part B: Atomic Spectroscopy, vol. 55, no. 7. Elsevier BV, pp. 1051–1061, Jul. 2000. doi: 10.1016/s0584-8547(00)00225-1.

[48] L. Han, M. L. Salum, K. Zhang, P. Froimowicz, and H. Ishida, “Intrinsic self-initiating thermal ring-opening polymerization of 1,3-benzoxazines without the influence of impurities using very high purity crystals,” Journal of Polymer Science Part A: Polymer Chemistry, vol. 55, no. 20. Wiley, pp. 3434–3445, Jul. 31, 2017. doi: 10.1002/pola.28723.

[49] A. H. Telli and J. Hacaloglu, “Effects of aromatic diboronic acid on thermal charateristics of polybenzoxazines based on phenol and aniline,” European Polymer Journal, vol. 108. Elsevier BV, pp. 182–190, Nov. 2018. doi: 10.1016/j.eurpolymj.2018.08.053.

[50] J. Hacaloğlu, T. Uyar, and H. Ishida, “Thermal Degradation Mechanisms of Polybenzoxazines,” Handbook of Benzoxazine Resins. Elsevier, pp. 287–305, 2011. doi: 10.1016/b978-0-444-53790-4.00059-x.

[51] K. Hemvichian and H. Ishida, “Thermal decomposition processes in aromatic amine-based polybenzoxazines investigated by TGA and GC–MS,” Polymer, vol. 43, no. 16. Elsevier BV, pp. 4391–4402, Jul. 2002. doi: 10.1016/s0032-3861(02)00281-1.

[52] I. Dueramae, C. Jubsilp, T. Takeichi, and S. Rimdusit, “High thermal and mechanical properties enhancement obtained in highly filled polybenzoxazine nanocomposites with fumed silica,” Composites Part B: Engineering, vol. 56. Elsevier BV, pp. 197–206, Jan. 2014. doi: 10.1016/j.compositesb.2013.08.027.

[53] G. Lazouzi et al., “Optimized preparation of alumina based fillers for tuning composite properties,” Ceramics International, vol. 44, no. 7. Elsevier BV, pp. 7442–7449, May 2018. doi: 10.1016/j.ceramint.2018.01.083.

[54] D.-Y. Li, Y.-S. Lin, Y.-C. Li, D.-L. Shieh, and J.-L. Lin, “Synthesis of mesoporous pseudoboehmite and alumina templated with 1-hexadecyl-2,3-dimethyl-imidazolium chloride,” Microporous and Mesoporous Materials, vol. 108, no. 1–3. Elsevier BV, pp. 276–282, Feb. 2008. doi: 10.1016/j.micromeso.2007.04.009.

[55] F. Wang, Z. Huang, Y. Qin, and Y. Li, “Thermal behavior of phenolic-based ceramizable composites modified by nano-aluminum oxide,” High Performance Polymers, vol. 28, no. 9. SAGE Publications, pp. 1096–1101, Jul. 28, 2016. doi: 10.1177/0954008315596800.

[56] G. R. Rao, I. Srikanth, and K. L. Reddy, “Effect of Organo Montmorillonite Nanoclay on Mechanical Properties Thermal Stability and Ablative Rate of Carbon fiber Polybenzoxazine Resin Composites,” Defence Science Journal, vol. 71, no. 5. Defence Scientific Information and Documentation Centre, pp. 682–690, Sep. 02, 2021. doi: 10.14429/dsj.71.16630.

[57] F. Xu, S. Zhu, Y. Liu, Z. Ma, and H. Li, “Ablation behavior and mechanism of TaSi2-modified carbon fabric-reinforced phenolic composite,” Journal of Materials Science, vol. 55, no. 20. Springer Science and Business Media LLC, pp. 8553–8563, Apr. 15, 2020. doi: 10.1007/s10853-020-04636-0.

[58] W. Yang et al., “Improving ablation properties of ceramifiable vitreous silica fabric reinforced boron phenolic resin composites via an incorporation of MoSi2,”

Plastics, Rubber and Composites, vol. 49, no. 10. SAGE Publications, pp. 456–469, Aug. 24, 2020. doi: 10.1080/14658011.2020.1808758.

[59]J. Ren, J. Dou, L. Zhang, S. He, Y. Qin, and H. Fu, “Enhancement of the Ablation Properties of Silica/Phenolic Resin Composites by SiC/Si 3 N 4 Multiphase Structures,” Journal of Macromolecular Science, Part B. Informa UK Limited, pp. 1–15, Jan. 31, 2024. doi: 10.1080/00222348.2023.2299906.

[60] Z. Eslami, F. Yazdani, and M. A. Mirzapour, “Thermal and mechanical properties of phenolic-based composites reinforced by carbon fibres and multiwall carbon nanotubes,” Composites Part A: Applied Science and Manufacturing, vol. 72. Elsevier BV, pp. 22–31, May 2015. doi: 10.1016/j.compositesa.2015.01.015.

[61] G. R. Rao, I. Srikanth, and K. L. Reddy, “Mechanical, thermal and ablative behavior of organo nanoclay added carbon fiber/cyanate ester resin composites and effect of heat flux on its ablative performance,” Polymers and Polymer Composites, vol. 29, no. 9_suppl. SAGE Publications, pp. S250–S261, Mar. 04, 2021. doi: 10.1177/0967391121998833.

[62] Y. Ling et al., “Construction of ‘Rigid-Flexible’ Cocrosslinked Networks by Grafting Bismaleimide and Silicone to Prepare Tough, Heat-Resistant, and Ablation-Resistant Epoxy Composites,” Industrial & Engineering Chemistry Research, vol. 63, no. 31. American Chemical Society (ACS), pp. 13623–13636, Jul. 24, 2024. doi: 10.1021/acs.iecr.4c02270.

[63] Y. Ji et al., “Synergetic effect of aramid fiber and carbon fiber to enhance ablative resistance of EPDM-based insulators via constructing high-strength char layer,” Composites Science and Technology, vol. 201. Elsevier BV, p. 108494, Jan. 2021. doi: 10.1016/j.compscitech.2020.108494.

[64] M. Guo, J. Li, K. Xi, Y. Liu, and J. Ji, “Effect of multi-walled carbon nanotubes on thermal stability and ablation properties of EPDM insulation materials for solid rocket motors,” Acta Astronautica, vol. 159. Elsevier BV, pp. 508–516, Jun. 2019. doi: 10.1016/j.actaastro.2019.01.047.

[65] W. Wang, L. Zhou, Y. Li, P. Li, G. Chen, and S. Yang, “Study on the Ablation Properties of Nano-graphite Modified EPDM Insulators,” Journal of Physics: Conference Series, vol. 2133, no. 1. IOP Publishing, p. 012019, Nov. 01, 2021. doi: 10.1088/1742-6596/2133/1/012019.

[66] M. Li, Y. Li, T. Hong, Y. Zhao, S. Wang, and X. Jing, “High ablation-resistant silicone rubber composites via nanoscale phenolic resin dispersion,” Chemical Engineering Journal, vol. 472. Elsevier BV, p. 145132, Sep. 2023. doi: 10.1016/j.cej.2023.145132.

[67] S. Shen et al., “Enhanced ablation resistance of Divinyl-POSS modified additional liquid silicone rubber and its fiber-reinforced composite,” Polymer Composites, vol. 43, no. 5. Wiley, pp. 2896–2908, Apr. 2022. doi: 10.1002/pc.26585.

[68] S. Shen et al., “Phosphazene derivative cross-linked liquid silicone rubber and its mechanical and thermal properties,” Polymer Degradation and Stability, vol. 203. Elsevier BV, p. 110086, Sep. 2022. doi: 10.1016/j.polymdegradstab.2022.110086.

[69] S. Zhao et al., “Curing mechanism, thermal and ablative properties of hexa-(4-amino-phenoxy) cyclotriphosphazene/benzoxazine blends,” Composites Part B: Engineering, vol. 216. Elsevier BV, p. 108838, Jul. 2021. doi: 10.1016/j.compositesb.2021.108838.

[70] H. C. Foley, M. S. Kane, and J. F. Goellner, “New Directions with Carbogenic Molecular Sieve Materials,” Fundamental Materials Research. Kluwer Academic Publishers, pp. 39–58. doi: 10.1007/0-306-47066-7_4.

[71] Z. Lule, H. Ju, and J. Kim, “Thermomechanical properties of alumina-filled plasticized polylactic acid: Effect of alumina loading percentage,” Ceramics International, vol. 44, no. 18. Elsevier BV, pp. 22767–22776, Dec. 2018. doi: 10.1016/j.ceramint.2018.09.066.

[72] M. Saleh, Z. Al-Hajri, A. Popelka, and S. Javaid Zaidi, “Preparation and Characterization of Alumina HDPE Composites,” Materials, vol. 13, no. 1. MDPI AG, p. 250, Jan. 06, 2020. doi: 10.3390/ma13010250.

[73] Y. Liu et al., “Silicone-based alumina composites synthesized through in situ polymerization for high thermal conductivity and thermal stability,” Materials Letters, vol. 261. Elsevier BV, p. 127002, Feb. 2020. doi: 10.1016/j.matlet.2019.127002.

[74] Y. Ouyang, G. Hou, L. Bai, B. Li, and F. Yuan, “Constructing continuous networks by branched alumina for enhanced thermal conductivity of polymer composites,” Composites Science and Technology, vol. 165. Elsevier BV, pp. 307–313, Sep. 2018. doi: 10.1016/j.compscitech.2018.07.019.

[75] R. Plengudomkit, M. Okhawilai, and S. Rimdusit, “Highly filled graphene-benzoxazine composites as bipolar plates in fuel cell applications,” Polymer Composites, vol. 37, no. 6. Wiley, pp. 1715–1727, Dec. 23, 2014. doi: 10.1002/pc.23344.

[76] B. Weidenfeller and M. Anhalt, “Polyurethane–magnetite composite shape-memory polymer,” Journal of Thermoplastic Composite Materials, vol. 27, no. 7. SAGE Publications, pp. 895–908, Oct. 09, 2012. doi: 10.1177/0892705712458446.

[77] A. Smirnov et al., “Structure formation and thermal conduction in polymer-based composites obtained by fused filament fabrication,” The International Journal of Advanced Manufacturing Technology, vol. 129, no. 5–6. Springer Science and Business Media LLC, pp. 2677–2690, Oct. 18, 2023. doi: 10.1007/s00170-023-12432-8.

[78] J. Xu et al., “Polyphenylene oxide/boron nitride–alumina hybrid composites with high thermal conductivity, low thermal expansion and ultralow dielectric loss,” Polymer Composites, vol. 45, no. 6. Wiley, pp. 5267–5280, Jan. 14, 2024. doi: 10.1002/pc.28125.

[79] C. Kittel, Introduction to Solid State Physics. Hoboken, NJ: Wiley, 2011. ISBN: 978-0-471-68057-4

APPENDICES

A. Autoclave Cure Cycle

The autoclave cure cycle given in Experimental section can be tabulated as Table A.1.

Table A.1. Autoclave cure cycle of polybenzoxazine composites

Time (min)	Temperature (°C)	Pressure (bar)
t_0	25	1
t_0+50	100	7
t_0+110	100	7
t_0+140	150	7
t_0+200	150	7
t_0+230	185	7
t_0+290	185	7
t_0+320	200	7
t_0+440	200	7
t_0+550	62.5	7
t_0+560	50	1

B. Viscosity of Uncured Polybenzoxazine Resin

The viscosity values of the uncured polybenzoxazine resin are found by performing viscometer tests with a tabletop Brookfield Rotating Viscometer at different temperatures and using different solvents to dilute the resin.

Table B.1. Viscosity values of benzoxazine resin at different temperatures

Temperature	**Viscosity (cP)**
25 °C	11200
40 °C	1170
60 °C	160

Table B.2. Viscosity values of benzoxazine resin in different solvents at 25 °C

Solvent and weight percent	**Viscosity (cP)**
3 wt% ethyl alcohol	3810
6 wt% ethyl alcohol	1540
9 wt% ethyl alcohol	710
3 wt% isopropyl alcohol	4640
6 wt% isopropyl alcohol	1640
9 wt% isopropyl alcohol	1150

C. Water Absorption Properties

One of the key properties of polybenzoxazine composites is their intrinsic low water absorption capacity [12] which is thought to be a beneficial feature regarding the service life of polybenzoxazine composite products. In this thesis, the water absorption limits of all polybenzoxazine composites are examined. These findings are illustrated in Figure C.1 and listed in Table C.1.

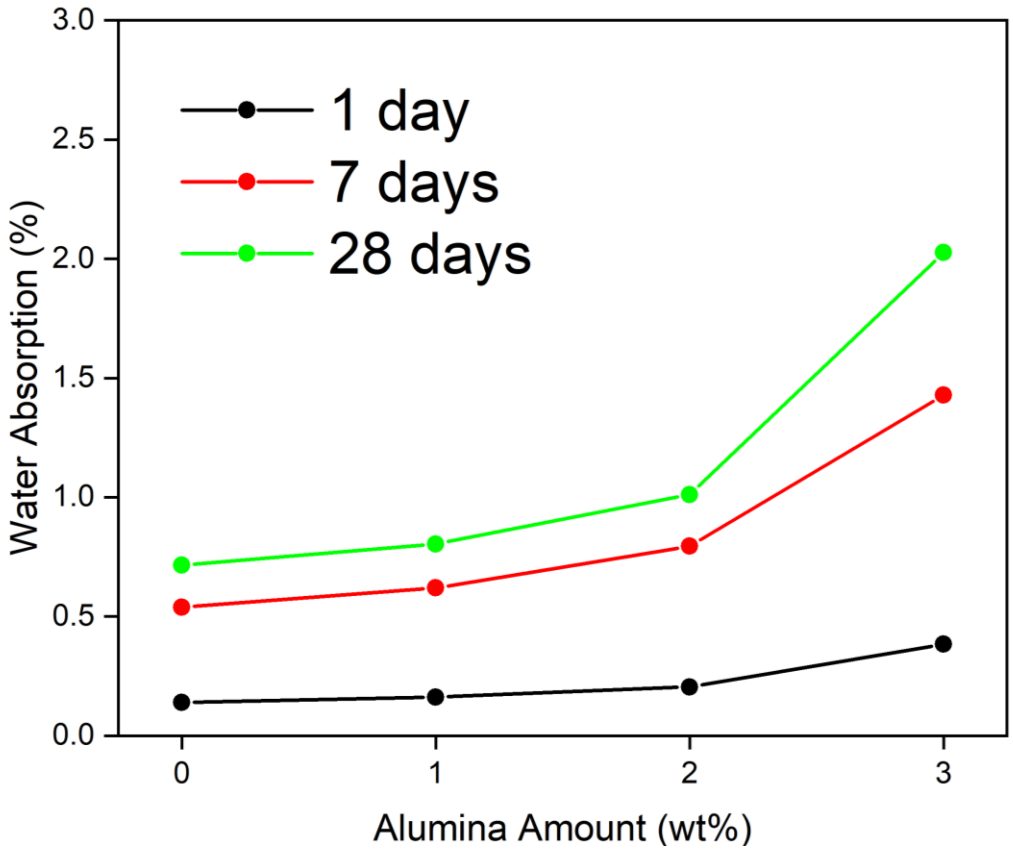

Figure C.1. Water absorption values of polybenzoxazine composites

Table C.1 The water absorption amounts of each composite

Composite Name	**Water Absorption (%)**	**Water Absorption (%)**	**Water Absorption (%)**
	1 day	**7 days**	**28 days**
PBZ0	0.1402	0.5395	0.7151
PBZ1	0.1623	0.6198	0.804
PBZ2	0.2046	0.795	1.0113
PBZ3	0.3834	1.4283	2.0258

D. Elemental Mapping Images

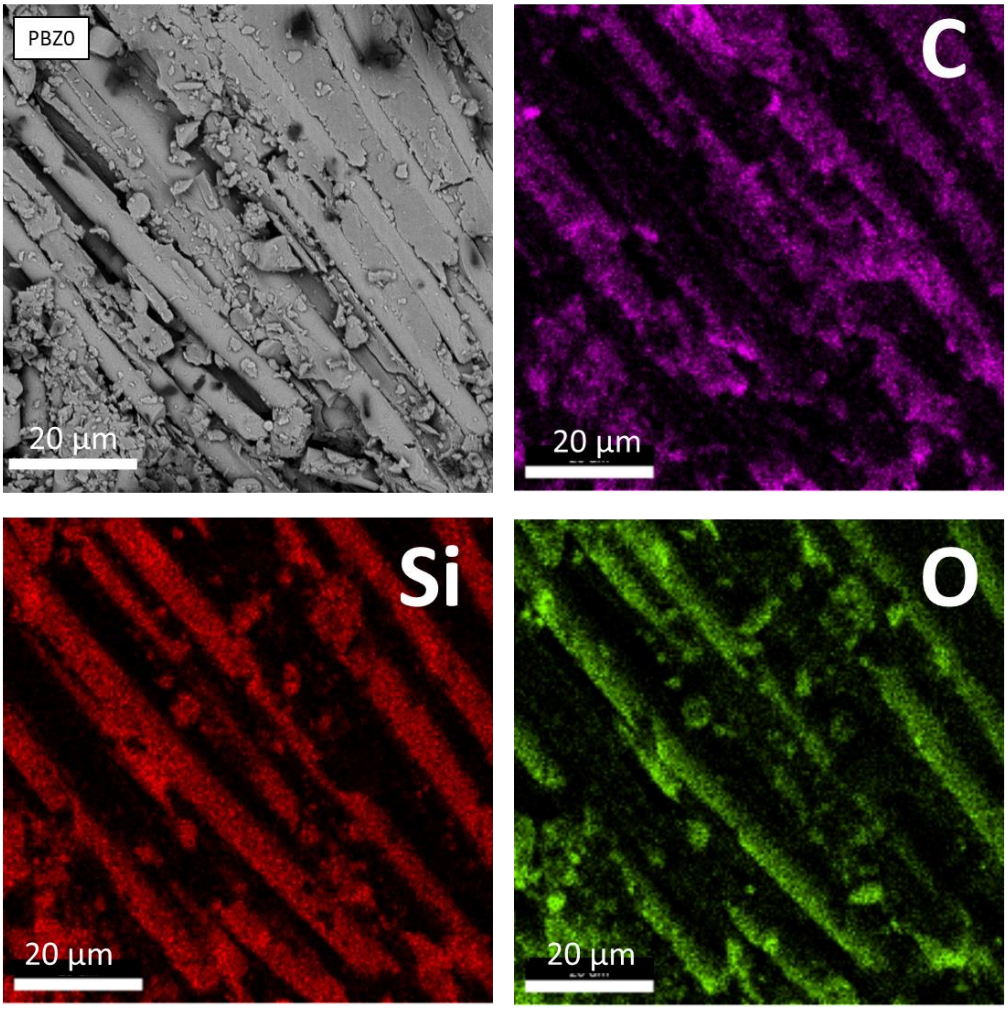

Figure D.1. Elemental mapping of polybenzoxazine composite PBZ0

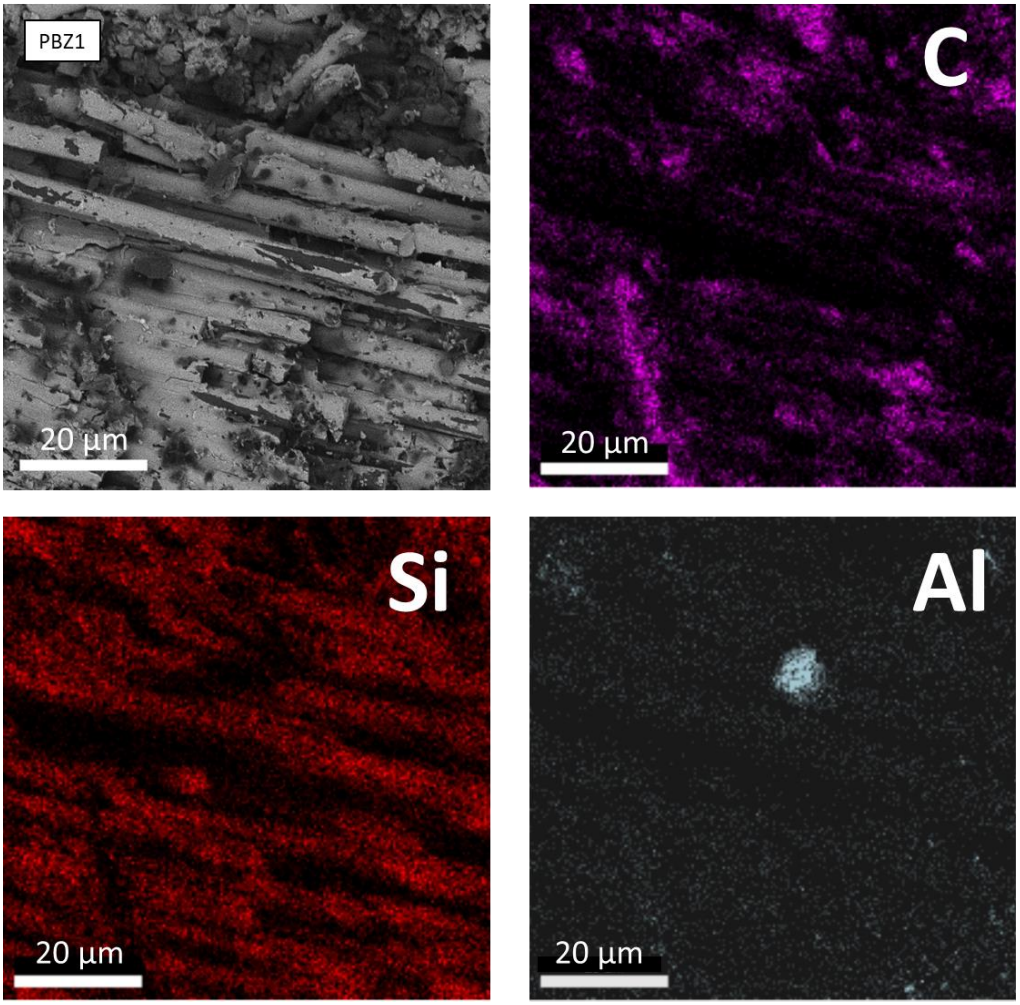

Figure D.2. Elemental mapping of polybenzoxazine composite PBZ1

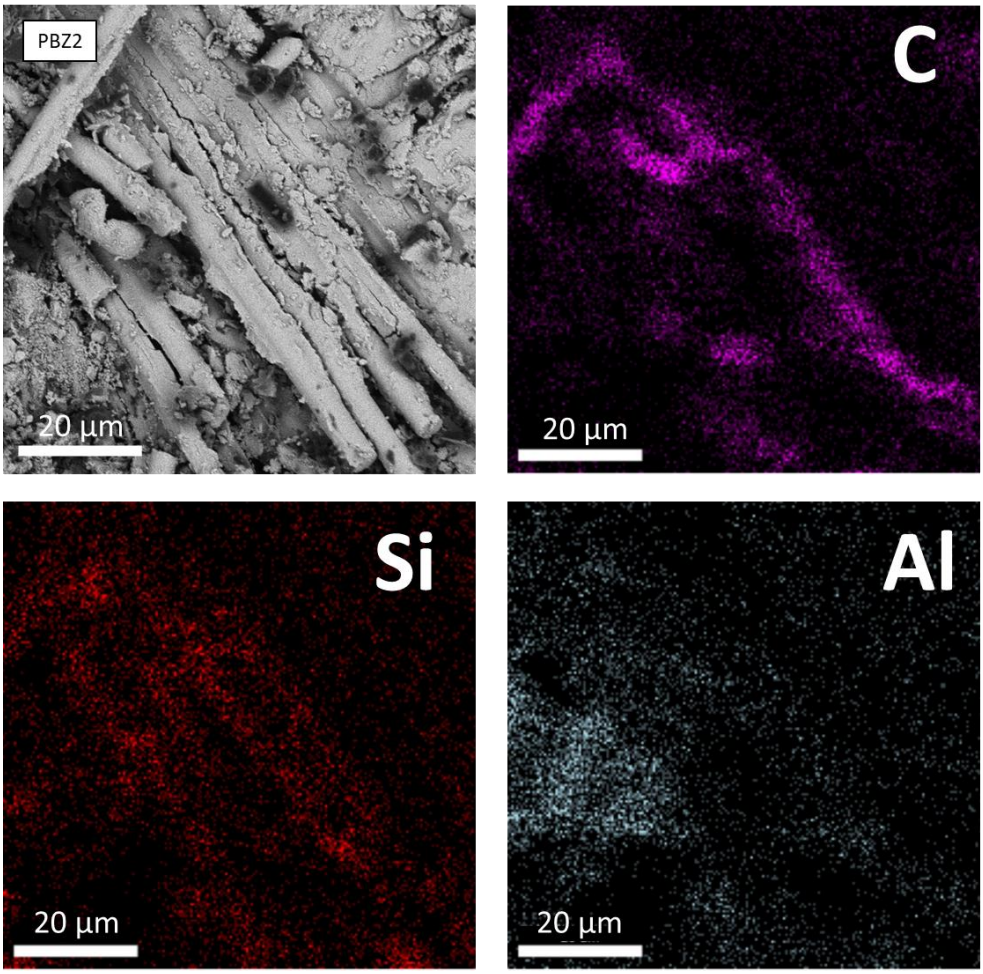

Figure D.3. Elemental mapping of polybenzoxazine composite PBZ2